Received: 3 August 2020 | Revised: 19 May 2021 | Accepted: 24 May 2021

DOI: 10.1002/dep2.155

ORIGINAL RESEARCH ARTICLE

The Depositional Record Open Access
A journal of the International Association of Sedimentologists
WILEY

The role of tectonic activity, topographic gradient and river flood events in the Testina travertine (Acque Albule Basin, Tivoli, Central Italy)

Fabio Scalera[1] | **Alessandro Mancini**[2] | **Enrico Capezzuoli**[3] | **Hannes Claes**[4,5] | **Rudy Swennen**[5]

[1]Primary and Secondary School, I.C, "Fratelli Cervi", Modena, Italy

[2]Department of Earth Sciences, University of Milan, "A. Desio", Milan, Italy

[3]Department of Earth Science, University of Florence, Florence, Italy

[4]Institute for Clay & Interface Mineralogy, EMR, Aachen, Germany

[5]Geology, Earth and Environmental Sciences, KU Leuven, Heverlee, Belgium

Correspondence
Alessandro Mancini, Department of Earth Sciences, University of Milan, "A. Desio", Via Mangiagalli 34, 20133 Milan, Italy.
Email: alessandro.mancini@unimi.it

Abstract

The Acque Albule Basin in Tivoli (Rome, Central Italy) represents one of the largest exposures of travertine deposits in the world. A detailed study of the Upper Pleistocene Testina travertine, constituting the poorly lithified top part of the *Lapis Tiburtinus* travertines, is presented. Fieldwork performed in an area of 10 km^2 and petrographic analysis allow the recognition of six geobodies with different geometries, degree of diagenetic alteration and architectural elements, composed of seven lithotypes. The Testina travertine appears in general as a poorly lithified travertine, even if it shows a high degree of cementation. It is mainly characterised by blocky, drusy or bladed microsparite and sparite calcite cements, related to thermal and meteoric phreatic to vadose water circulation, affecting in particular those travertine deposits located in the northern part of the study area. The Testina, neglected until now in the several studies performed in the Acque Albule Basin, shows a progradational trend from the north to the south and is characterised by environments, evidencing deposition on a gentle slope, in an alluvial plain and in a shallow lake, with gradual transitions between low-energy environments and high-energy environments. Furthermore, based on correlation between the different geobodies in the overall study area, the Testina travertine depositional system was influenced by tectonic activity in the northern part, by an increasing topographic gradient and water discharge flow in the central part and by flooding events related to the Aniene River in the southern part. This study aims to differentiate such influencing factors facilitating the analysis of other travertine depositional systems and also to aid in the interpretation of subsurface analogues, as in the case of South Atlantic Pre-Salt reservoirs.

KEYWORDS

Acque Albule Basin, Aniene River, depositional system, Late Pleistocene, travertine

1 | INTRODUCTION

Travertine deposits are composed of a wide variety of lithotypes, each with different petrographic and geochemical features (Capezzuoli et al., 2014; Chafetz & Folk, 1984; Gandin & Capezzuoli, 2014; Guo & Riding, 1998; Özkul et al., 2002; Pedley & Rogerson, 2010; Pentecost, 2005; Toker et al., 2015) as well as complex depositional units characterised by high lateral and vertical heterogeneities (Della Porta, 2015, 2017a, 2017b; Guo & Riding, 1998, 1999). Quantitative information on dimensions, shapes and orientations of the different travertine geobodies is important to better understand the depositional environments where these deposits developed (Mancini et al., 2019a).

Based on Capezzuoli et al. (2014), travertine deposits are continental limestones forming where hydrothermal and meteoric groundwater reach the surface. The carbon dioxide outgassing causes the rapid precipitation of travertine (Mancini et al., 2019a, 2019b; Pentecost, 2005), resulting in complex configurations of the resulting geobodies. Furthermore, most of these geobodies generally reflect the interaction between biotic and abiotic processes (Brasier, 2011). Travertine deposits have been studied worldwide by many authors as for example in Central Italy (Brogi, 2004; Brogi et al., 2012, 2020; Capezzuoli et al., 2014; Janssens et al., 2020; Minissale, 2004), the Denizli Basin in Turkey (Aratman et al., 2020; Brogi et al., 2014, 2016; Claes et al., 2015; Claes et al., 2017b; De Boever et al., 2016; De Boever et al., 2017b; Mohammadi et al., 2020; Özkul et al., 2002), the Mammoth Hot Springs at Yellowstone, USA (Fouke, 2011; Fouke et al., 2000) and in Hungary (Claes et al., 2017a; Claes et al., 2020; Török et al., 2017, 2019).

The *Lapis Tiburtinus* travertine deposits have been studied by several authors over the last 40 years (Anzalone et al., 2017; Chafetz & Folk, 1984; Della Porta et al., 2017a; De Filippis et al., 2012; De Filippis et al., 2013a, 2013b; Erthal et al., 2017; Faccenna et al., 2008; Mancini et al., 2019a). The name 'travertine', in fact, originates from the Latin words *Lapis Tiburtinus*, where *Lapis* means rock, while the term *Tiburtinus* refers to the ancient town of *Tibur* (Tivoli at the present day; Chafetz & Folk, 1984).

The so called Testina, representing the youngest carbonates at the top of the succession of the *Lapis Tiburtinus* travertine (29 ± 4 ka, Faccenna et al., 2008), consists of a poorly lithified and porous travertine, capping most of the Acque Albule Basin with an average thickness of 8 m (De Filippis et al., 2013a). A detailed sedimentological study was carried out in an area of 10 km^2. Tectonic activity and climate variations are fundamental in travertine formation, because they influence the groundwater table, the position of the springs and the geometries of travertine geobodies (Anzalone et al., 2017; De Filippis et al., 2013a, 2013b; Faccenna et al., 2008). The influence of such factors in the *Lapis Tiburtinus* travertine succession was investigated in the underlying deposits and reported by several authors (Della Porta et al., 2017a; Faccenna et al., 2008), but never in the Testina travertine.

Over the last several years, interest in continental carbonates has increased both in the academic world and in the oil industry, due to the discovery of South Atlantic Pre-salt carbonate reservoirs (Brazil and Angola—Saller et al., 2016; Terra et al., 2010) that display similarities with travertines (Alvarenga et al., 2016; Basso et al., 2020). In the framework of the Pre-salt carbonate reservoirs discovered in Brazil and Angola, interpreted as lacustrine freshwater to alkaline deposits (Sabato Ceraldi & Green, 2016; Saller et al., 2016; Wright & Barnett, 2015) and sometimes associated with travertines derived from vents or spring mounds (Alvarenga et al., 2016), the study of exposed reservoir analogues is fundamental to assess reservoir architecture (Casanova, 1994; Della Porta, 2015; Jones & Renaut, 1995; Mancini et al., 2019a; Renaut et al., 2013). Therefore, many authors, based on sedimentological analysis, suggest the use of continental carbonate depositional systems as possible analogues of Pre-salt reservoirs (Bosence et al., 2015; Claes et al., 2015; Claes et al., 2017a; Della Porta et al., 2017b; Erthal et al., 2017; Mancini et al., 2019a; Ronchi & Cruciani, 2015; Soete et al., 2015; Török et al., 2017). Such reservoirs are characterised by the presence of shrub-like fabrics (Dias, 2004; Rezende & Pope, 2015; Terra et al., 2010), representing for many authors one of the most important targets for oil exploration due to the associated high permeability (Wright, 2012; Wright & Barnett, 2015). Despite the crystalline composition of the Pre-salt shrubs, these deposits are morphologically similar to the shrub boundstone described in the Testina travertine (Basso et al., 2020; Claes et al., 2017b; Chafetz & Folk, 1984; Erthal et al., 2017; Guo & Riding, 1998), and for this reason this study can provide useful information to better understand the spatial distribution of shrub lithologies in subsurface reservoirs.

2 | GEOLOGICAL SETTING

2.1 | Regional setting

Central Italy (Figure 1), and in particular the Apennine belt, is characterised by Meso-Cenozoic carbonates and evaporite deposits organised in a system of thrust sheets, eastward-migrating from the Late Miocene until the Pliocene (Billi & Tiberti, 2009; Billi et al., 2006; Cavinato & De Celles, 1999; Patacca et al., 1992). From the Late Miocene to Pliocene the western part of the Apennine belt was characterised by the activation of normal faults related to a back-arc tectonic regime, while in the eastern part accretion was still active on the frontal part of the orogenic belt (Carmignani et al., 1994;

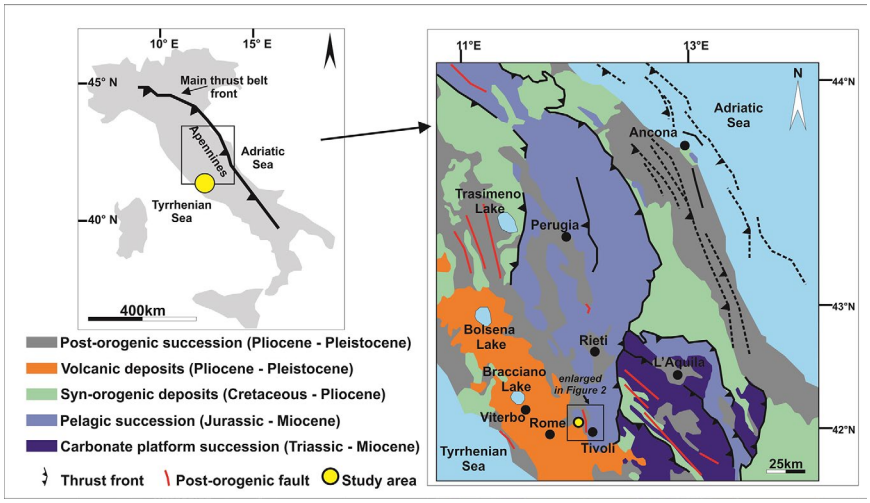

FIGURE 1 Geological map of Central Italy. The black square of the geological map represents the study area, reported in Figure 2A. (modified after Vignaroli et al., 2019)

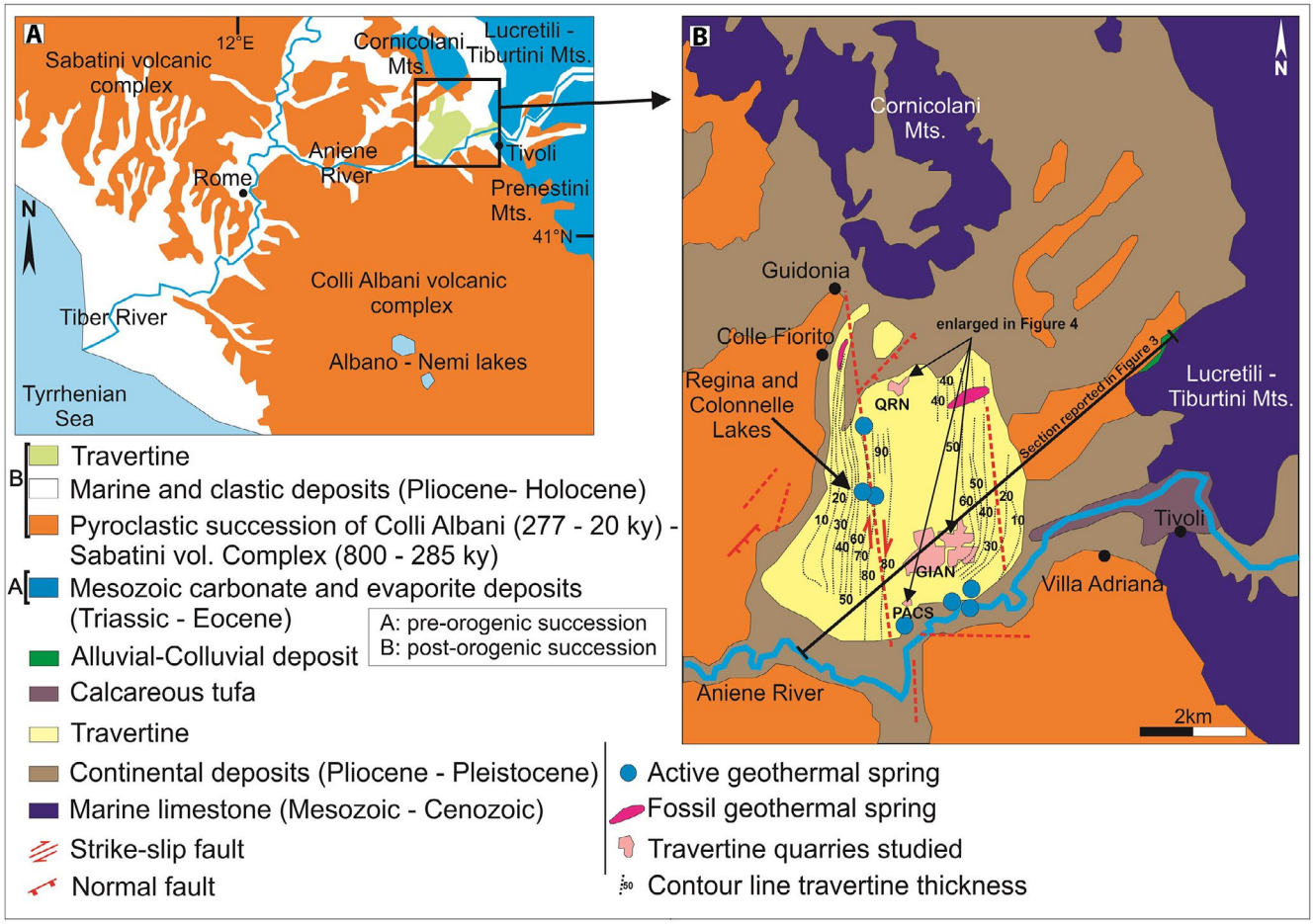

FIGURE 2 (A) Synthetic geological map of the Roman Basin (modified after Milli et al., 2016). (B) Geological map of the Acque Albule Basin indicating the major faults and springs present in the area. Notice that springs are located in proximity of the major structural features (modified after Faccenna et al., 2008; Giordano et al., 2010; De Filippis et al., 2013a)

Carminati & Doglioni, 2012; Molli, 2008; Patacca et al., 1992; Rossetti et al., 2015). The western part of the Apennine belt, the present-day Tyrrhenian side, is characterised by several sedimentary basins mainly associated with a system of NW–SE striking normal faults. The age of the deposits filling these sedimentary basins reveals that growth of normal faults occurred during the Miocene-Early Pleistocene (Faccenna et al., 2008; Liotta, 1991). Furthermore, other effects of such extensional process in the western side are represented by the reduced thickness of the lithosphere, the presence of a high

heat flow, the occurrence of several Pliocene–Quaternary basins and by the presence of magmatic districts, all oriented along the western portion of the Apennine belt (Acocella & Funiciello, 2006; Brogi et al., 2005; Dini et al., 2005; Liotta & Brogi, 2020; Serri et al., 1993). One of these districts includes the Colli Albani quiescent volcanic complex and the adjacent peri-volcanic hydrothermal area of the Acque Albule Basin (De Rita et al., 1995, 2002; Faccenna et al., 2008; Gaeta et al., 2000; Karner et al., 2001).

2.2 | The Acque Albule Basin

The Acque Albule Basin (Pleistocene; Faccenna et al., 2008) is located 30 km to the east of Rome covering an area of 28 km^2 to the west of Tivoli city (Figure 2A). This basin is confined to the north and east by the Apennine belt, to the south by the Aniene River and the Pleistocene Colli Albani volcanic complex and to the west by the Roman Basin (Milli et al., 2016). The Acque Albule Basin is a morphological depression overlying a thick (4–5 km at least) succession of Meso-Cenozoic marine carbonate rocks (Faccenna et al., 2008) and filled by Plio-Pleistocene alluvial, lacustrine and epivolcanic deposits. The top of this sedimentary succession is characterised by the presence of the *Lapis Tiburtinus* travertine (Della Porta et al., 2017a; Faccenna et al., 2008), deposited after or concurrently with the last phase of Colli Albani volcanic activity (Late Pleistocene time; Faccenna et al., 2008; Gaeta et al., 2000). The *Lapis Tiburtinus* travertine succession developed between 115 and 30 ka (Late Pleistocene; Faccenna et al., 2008) and is characterised by travertine units with a gentle inclination (3°–4°) from the north toward the south and from the east toward the west. The Late Pleistocene–Holocene tectonic activity of the area is, according to Faccenna et al. (2008) and De Filippis et al. (2013a) and De Filippis et al. (2013b), different from the previous extensional regime and mainly characterised by N–S striking, transtensional-to-normal faults, which caused part of the subsidence of the Acque Albule Basin through a pull–apart mechanism (De Filippis et al., 2013a). These structures have partially controlled the latest stages of volcanism and the related hydrothermal outflows (Faccenna et al., 2008). The main N–S strike-slip fault is documented on outcrops of the Cornicolani Mountains, immediately to the north of the basin, whereas the fault southward prolongation beneath the basin coincides with the two main (Figure 2B) thermal springs of the area (i.e. Regina and Colonnelle Lakes; Faccenna et al., 2008). Some of these faults are still active (or they are activated by pore pressure increase; Billi et al., 2007), as demonstrated by the low-magnitude (2.1–2.7), shallow (less than 1.5 km), seismic event in 2001 beneath the Acque Albule Basin (De Filippis et al., 2013b).

2.3 | Previous studies on the sedimentology of the *Lapis Tiburtinus* travertine

As reported in Della Porta et al. (2017b), since the 1980s the *Lapis Tiburtinus* deposits have attracted the interest of several authors. In the study performed by Chafetz and Folk (1984), *Lapis Tiburtinus* deposits were attributed to a depositional system related to an extensive and laterally continuous lacustrine setting, characterised by the predominance of shrub lithofacies, sometimes interrupted by the higher energy conditions associated with lithofacies containing calcite ray-crystals, intraclasts and pisoids. Successively, the *Lapis Tiburtinus* deposits were attributed by Pentecost (2005) to an irregular mound, affected by topographic gradient with low relief depositional system, organised into sheet-like layers gently dipping toward the Aniene River.

According to Faccenna et al. (2008), 70% of the *Lapis Tiburtinus* travertine deposited inside the Acque Albule Basin is associated with water circulating in the thermal springs and flowing toward the Aniene River, producing five tabular subhorizontal units 8–10 m thick and interrupted by erosional surfaces. Faccenna et al. (2008) and De Filippis et al. (2013a) suggested that the erosional surfaces are related to water table fluctuations, influenced by the Pleistocene palaeoclimate variations of the last 150 kyr as well as fault-related deformations and volcanic activity associated with the Colli Albani volcanic complex.

De Filippis et al. (2013a) described, in the north-west sector of the *Lapis Tiburtinus* deposits (Colle Fiorito area), a 2 km long and nearly 15 m high fissure-ridge structure, controlled by fluctuations of the groundwater table. The *Lapis Tiburtinus* was described as a travertine succession reaching a maximum thickness of 80–90 m related to a N–S striking fault and defined as a morphological structure without a prominent topography called 'travertine plateau' (De Filippis et al., 2013b). The water discharge represents, according to De Filippis et al. (2013b), the most important factor keeping open the fractured conduits feeding the travertine deposits, activating the faults and the subsidence of the entire area.

Erthal et al. (2017) suggested that the *Lapis Tiburtinus* deposits are related to an extensive waterlogged flat setting laterally varying into a slope system. The entire depositional system is influenced by water flow hydrodynamic conditions, CO_2 degassing rate, evaporation and influence of microbially mediated precipitation.

Based on sedimentological, stratigraphical and geochemical data collected from a 30 m thick borehole drilled in the north-west quarried area, Anzalone et al. (2017) suggested that the *Lapis Tiburtinus* deposits formed in a shallow lake and slope depositional setting affected by the presence of cyclical erosional discontinuities, related to climate fluctuations

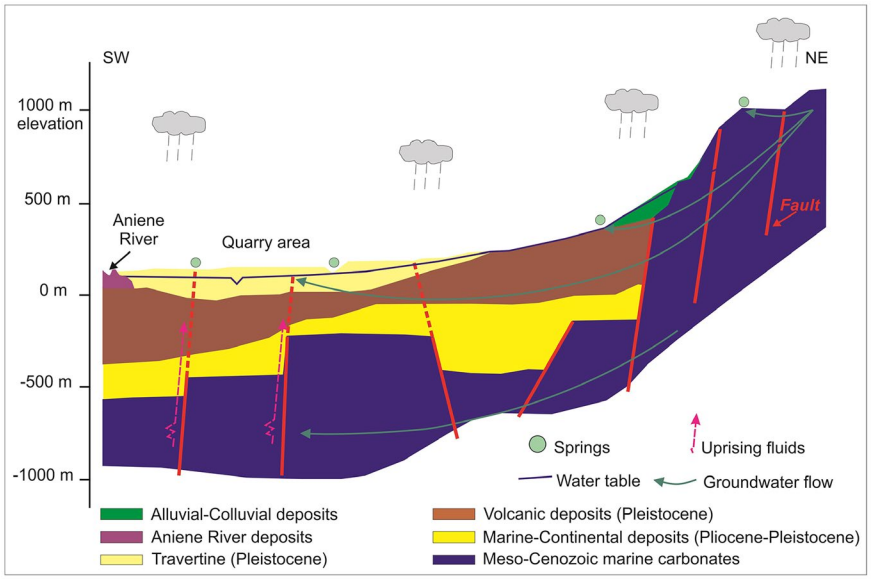

FIGURE 3 Hydrogeological model of the Acque Albule Basin (modified after Carucci et al., 2012; Della Porta et al., 2017a)

of Milankovitch orbital forcing, influencing the water table fluctuations.

According to Della Porta et al. (2017a), the *Lapis Tiburtinus* deposits can be divided into three different depositional zones: (a) a proximal zone in the north, close to the spring area, characterised by deposition in horizontal to gently dipping pools evolving into a low angle terraced system; (b) an intermediate zone in a smooth to terraced slope setting dipping 5°–40° toward the southern and eastern sectors; (c) a distal zone composed of lobes dipping toward the south and developing into a smooth terraced system, alternating with alluvial to fluvial terrigenous deposits.

The nine different units identified by Della Porta et al. (2017a) in the *Lapis Tiburtinus* are characterised by a wedge-shaped geometry with variable lateral thicknesses (5–10 m) and bounded by unconformities related to erosive or non-depositional periods, suggesting that the entire depositional system was controlled by changes in the location of the active vents, intermittent vent activity, topographic gradient, rates of thermal water discharge and rates of carbonate precipitation.

Mancini et al. (2019a) classified and divided the entire *Lapis Tiburtinus* depositional system into three different zones, based on a hierarchical approach. The proximal zone is located in the northern part of the area (Colle Fiorito hill; De Filippis et al., 2012) and is represented by a fissure-ridge element with a ridge shape. The intermediate zone is occupied by a slope element with a very gentle inclination (from sub-horizontal up to 7°–10°) with sheet, pool and channel depositional settings and facies dominated by biotic crusts. Finally, a distal zone is formed by marshes and alluvial plain elements with a sheet shape crossed by channels and mainly characterised by biotic crusts and lithoclastic deposits.

The topmost part of this compact hydrothermal travertine succession consists of scarcely lithified, mixed carbonate–siliciclastic facies known as Testina (Faccenna et al., 1994, 2008), overlooked by the several scientific studies performed in the area. Such deposits represent the last depositional stage of the Acque Albule Basin which started around 29 ± 4 ka based on a U/Th dating performed by Faccenna et al. (2008).

2.4 | Hydrogeological framework

The Acque Albule Basin is characterised by a hydrogeological system composed of two connected aquifers, as also evidenced in Della Porta et al. (2017a) (Figure 3). The deeper one is represented by fractured Mesozoic–Cenozoic limestone and evaporitic strata, while the shallowest one, is unconfined to semi-confined within the Late Pleistocene travertine deposits (Carucci et al., 2012; La Vigna et al., 2013a, 2013b, 2016; Petitta et al., 2010). Discontinuous Pliocene marine claystone deposits of low permeability divide the two aquifers which are capped by the Pliocene–Pleistocene continental siliciclastic to volcanic deposits that constitute the aquiclude (Di Salvo et al., 2013; La Vigna et al., 2013a). Tectonic discontinuities connect the two aquifers as well as upwelling deep, high temperature CO_2-rich mineralized water which mixes with the shallow ambient temperature meteoric water coming from the carbonate ridges (Carucci et al., 2012; De Filippis et al., 2013a; Mancini et al., 2019a; Minissale et al., 2002). The several springs of the area discharge water with a temperature of 23°C, a pH of 6.0–6.2 and a pCO_2 of 0.6 atm (Maiorani et al., 1992; Minissale, 2004; Minissale et al., 2002) (see Regina and Colonelle Lakes in Figure 2B) and geothermal heat, related to the Colli Albani volcanic complex (Billi et al., 2007; Di Salvo et al., 2013; Faccenna et al., 2008; Minissale et al., 2002). The Ca-Mg-HCO_3 composition

of the local spring fluids is related to the decarbonation of Mesozoic–Cenozoic carbonates while the high concentration of sulphate is caused by leaching of the Triassic evaporite deposits of the Burano Formation (Minissale, 2004; Minissale et al., 2002). The shallow travertine aquifer is directly fed by rainwater from the surrounding carbonate ridges with a drainage path provided by the Aniene River, in the southern part of the Acque Albule Basin (Carucci et al., 2012; Di Salvo et al., 2013; La Vigna et al., 2013a, 2013b; Petitta et al., 2010).

3 | METHODS

Field observations were performed in an area of 10 km^2, analysing the well-exposed outcrops in the northern, central and southern sector of the quarried area, where the Testina travertine exposure is up to 8 m in thickness. Photographs of the whole quarry walls were printed and used in the field for detailed line drawings, allowing assessment of the thickness, lateral continuity and variations of each geobody.

The different geobodies composing the Testina travertine and their bounding surfaces were reconstructed applying the principles of synthem stratigraphy and related with the Unconformity-Bounded Stratigraphic Units (UBSUs; Chang, 1975; allostratigraphy; NACSN, 1983).

The UBSUs are stratigraphic units allowing the characterisation of sedimentary bodies in areas affected by cyclical phenomena, such as tectonic activity and climate-driven sea-level changes. The units can be classified as rock units bounded by unconformity surfaces.

The fabric type description and the travertine classification already applied in previous studies (Chafetz & Folk, 1984; Gandin & Capezzuoli, 2014; Guo & Riding, 1998; Della Porta, 2015; Della Porta et al., 2017a, 2017b; Özkul et al., 2002) is here used and integrated with the classification of carbonate textures (Dunham, 1962; Embry & Klovan, 1971). Detailed stratigraphic logs with sedimentological characterisation of the succession were acquired in three different quarries, chosen as the most representative of the different parts of the study area (Figure 4). The first log was realised in the northern part at the QRN quarry and consists in a vertical section comprising 7.5 m of unlithified Testina travertine and 4.4 m of the underlying *Lapis Tiburtinus*, totalling 11.9 m in thickness. The second log was measured in the GIAN quarry, typifying the central part, with a total vertical thickness of 8.5 m, including 1.4 m of the underlying *Lapis Tiburtinus*. The last three stratigraphic logs were performed in the southern part in the PACS quarry, over a total thickness of 9.4 m, comprising 2.5 m of the *Lapis Tiburtinus*.

A total of 31 samples were doubly impregnated with resin before thin section preparation due to the fragility of travertine, particularly at pore edges. A fluorescent dye was used in order to easily distinguish micro-porosity with

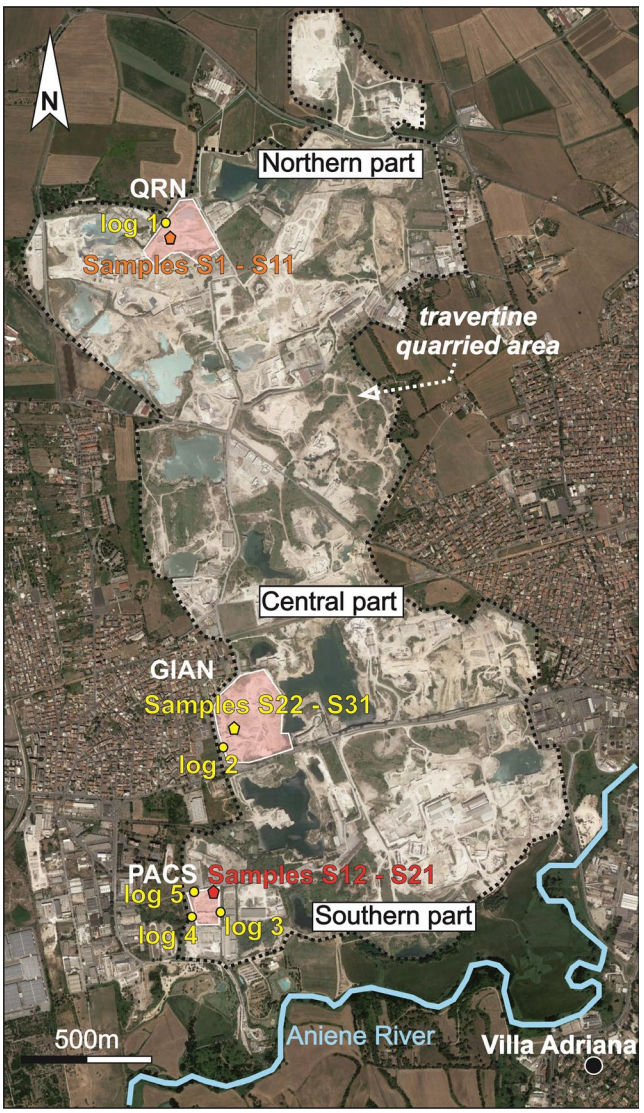

FIGURE 4 Map of the studied quarries. The position of the stratigraphic logs and samples collected is also indicated (QRN: Querciolaie quarry; GIAN: Giansanti quarry; PACS: Pacifici quarry). The yellow dots indicate the exact log positions (maps modified from Google Earth, Digital Globe, 2020)

fluorescent light microscopy. The petrographic characterisation was performed on an Olympus BX60 (Olympus Corporation) and Leica (Leica Microsystems) DM LP microscope. A Zeiss Axio Imager Z1m microscope with adapted filter set (EX BP365/12 EM LP397, EX G 365 EM LP 420 and EX BP 450-490 EM LP 515) was used to take pictures of the different samples analysed. Thin sections were also treated with alizarin red S (ARS) and potassium ferricyanide (PF) dissolved in a dilute hydrochloric acid solution, in order to distinguish ferroan calcite from non-ferroan calcite and dolomite (Dickson, 1966). Thin sections were soaked in the solution for a period of 30 s and subsequently washed with distilled water and dried well to remove impurities. Cathodoluminescence analysis was performed with a Nikon Optiphoto with a modified Techosyn

Model 8200 MARK II. Samples were then inserted in a vacuum chamber with a low vacuum varying between 35 and 43 mTorr. The electron beam has a width of 5 mm and hits the sample at a shallow angle. The voltage used varied between 7 and 8 kV and the current between 200 and 300 mA.

4 | RESULTS

4.1 | Lithotypes description

Seven lithotypes labelled microbial laminite, shrub boundstone, crystalline crust, lithoclast travertine, reed travertine, peloidal micrite and silt with clasts are identified in the studied quarries, reflecting sedimentation processes that can be linked to specific depositional settings. The lithotypes were distinguished based on meso-scale to micro-scale characteristics and depositional geometry. In the proposed travertine lithotype description, the term 'interlaminar porosity' refers to Claes et al. (2017b). A summary of the descriptions is given in Table 1.

4.1.1 | Microbial laminite

Description: Microbial laminite is mainly characterised by tabular and lenticular geometries, with a maximum thickness of 2 m. It is one of the most recurrent lithotypes within the studied sections. The texture is characterised by vacuolar networks, comprising whitish to pale brown coloured laminae up to 4 mm in thickness, reflecting an alternation of micrite and sparite (Figure 5A1, A3). These laminae show mainly sub-horizontal stratification with some minor undulations. At micro-scale, microbial laminite is mostly characterised by clotted micrite, often strongly cemented by blocky calcite cement. This lithotype shows fenestral to interlaminar porosity, clearly recognisable at macroscopic and microscopic scale. The abundant blocky calcite cement usually fills the primary porosity occurring between the clotted micrite (Figure 5A2, A4, A5). Locally, lenticular shaped vacuoles resembling Chironomid larval tubes (Figure 5A2) occur.

Interpretation: Microbial laminite usually forms under low-energy conditions (Gandin & Capezzuoli, 2014), such as pools in terraced slope systems (Guo & Riding, 1999) and are principally interpreted as being precipitated by microbially mediated processes (Gandin & Capezzuoli, 2014). The laminae are characterised by variations of white and dark colours, resembling alternating heteropachous lamination sensu Pentecost (2005). The whitish layers may have precipitated mainly inorganically, while the dark layers correspond to the incorporation of organic components (Erthal et al., 2017). According to Toker et al. (2015), alternating laminae could be related to seasonal variations and/or biological activity. A comparable lithotype to the microbial laminite observed in the Testina have been reported by Guo and Riding (1999), Rainey and Jones (2009), Gandin and Capezzuoli (2014), Claes et al. (2015), Claes et al. (2017a) and Croci et al. (2016), from different localities such as the Denizli Basin (Turkey) and Tuscany (Italy). This lithotype forms under slow flowing, weakly agitated spring water or reduced water discharge conditions related to microbially mediated processes (Rainey & Jones, 2009). Flat to slightly undulated microbial laminite can be observed in very shallow pools where micritic lime-mud accumulates at the bottom as a blanket over thin films of bacterial colonies and their mucilaginous extracellular polymeric substances (EPS), forming sheets that rapidly acquire a leathery consistency (Gandin & Capezzuoli, 2014). This process appears to be triggered by steady evaporation that gives rise to whitings and deposition of minor quantities of micrite mud and then to syneresis processes driven by variations in fluid density and concentration, that leads to dehydration of the microbial components of the sediment with deformation and/or cracking of the carbonate sheets (Gandin & Capezzuoli, 2014).

4.1.2 | Shrub boundstone

Description: The shrub boundstone lithotype has a thickness of 2 m with tabular geometries, consisting of a boundstone texture characterised by lamination encapsulating bush-like growth structures (Figure 5B1, B3). These bush-like structures are entirely bounded by micritic layers. Shrub boundstone shows a sub-horizontal lamination of a whitish to beige colour at meso-scale with laminae thickness of about 1 mm. In detail, these fabrics possess a well-defined morphology consisting of a clear vertical stem with small and narrow branches expanding upward with narrow and tight packing (Erthal et al., 2017). At micro-scale, this lithotype consists both of micrite and blocky calcite cement, the latter often micritized. Micrite occurs in sub-horizontal layers of 0.5–1 mm, while blocky cement usually surrounds the shrub structures, thus reducing the porosity related to this lithotype. The dense micritic layers mainly consist of clotted micrite characterised by low porosity, while the narrow shrubs possess some well-developed porosity related to inter-shrub porosity (Figure 5B2, B4, B5).

Interpretation: Shrub boundstone lithotypes commonly develop in low-energy environments, such as shallow water lakes and shallow pools, subject to biologically harsh conditions (for example in the proximity of H_2S-rich springs) (Chafetz & Folk, 1984; Erthal et al., 2017). The shrub structures themselves formed mainly under microbial influence and the upward orientation is due to the hard surfaces located below, preventing downward growth (Erthal et al., 2017).

TABLE 1 Lithotype descriptions of the Testina travertine

Lithotype name	Description	Geometry and thickness	Microscopic and diagenetic features	Porosity type	Depositional environment	Lithotype association
Microbial laminite	Microbial boundstone (sensu Della Porta et al., 2017b) characterised by whitish to pale brown-coloured laminae up to 4 mm in thickness. Laminae reflect the alternation of micrite and sparite Chironomid larval tubes	Tabular and lenticular geometries, with a maximum thickness of 2 m for each layer	Microbial lamine formed by clotted micrite, often strongly cemented by blocky calcite cement. Abundant blocky cement usually filling the primary porosity occurring between the clotted peloidal micrite	Fenestrae to interlaminar porosity	Shallow pools and pans characterised by slow flowing, weakly agitated spring water or reduced water discharge conditions with microbially mediated processes. Alternation of white and dark layers reflect seasonal variations of the climate and/or biological activity	Shallow lake. More diffused in the southern sector of the study area
Shrub boundstone	Boundstone characterised by sub-horizontal lamine of *ca* 1 cm whitish to beige coloured, encapsulating bush-like growth structures. Shrubs possess a well-defined morphology consisting of a clear vertical stem with small and narrow branches expanding upward	Tabular geometries with a thickness of *ca* 2 m for each layer	Dense micritic layers mainly consist of clotted micrite characterised by sub-horizontal layers of 0.5 to 1 mm. Blocky cement appears often micritized	Micritic layers characterised by low porosity. Narrow shrubs possess some well-developed inter-shrub porosity	Shallow water lakes and shallow pools related to low-energy environments, probably influenced by microbial activity during evaporation phenomena	Shallow lake. Particularly abundant in the northern and central part of the study area
Crystalline crust	Cementstone (sensu Della Porta, 2015; Della Porta et al., 2017b) consisting of alternating micritic and dense crystalline laminae that are commonly, crudely fibrous with a bright white colour. Crusts are made of composite calcite crystals with feather-like structures developing perpendicular to the depositional surface	Tabular and lenticular with a thickness from 2 to 3 m. The dimensions of crystalline crusts change from few millimetres to 5 cm in thickness	Micritic laminae commonly dark-coloured and sparite laminae. Feather calcite crystals are often micritized	Porosity can develop between laminae (interlaminar porosity) or between crystals as growth-framework porosity	High-energy environments. The crusts commonly form as the result of rapid precipitation from fast flowing waters on smooth slope, rims and vertical walls of terrace pools, cliff surface of waterfall sub-environments	Slope. Represented in each analysed section above an erosional surface

(Continues)

TABLE 1 (Continued)

Lithotype name	Description	Geometry and thickness	Microscopic and diagenetic features	Porosity type	Depositional environment	Lithotype association
Lithoclast travertine	Packstone to floatstone with a beige to dark grey colour, characterised by the abundant presence of sub-angular to sub-rounded white coloured clasts with a diameter up to 1 cm. Peloids and gastropods	Sub-horizontal tabular geometries with layers up to 40 cm thick	Microsparite and drusy, blocky or eventually bladed cement, usually strongly micritized and often filling the vugs	Vugs. Micritic areas show partially cemented pores	Shallow pools, ponds, micro to macro terrace depositional system, characterised by low energy water flow. Distal, palustrine depositional setting in shallow or ephemeral ponds	Alluvial plain. Mainly recurrent in the lower part of section of the northern area
Reed travertine	Boundstone beige to brownish coloured characterised by in situ moulds of reed bushes, encrusted in life position by calcite, and coarse plant stem moulds up to 2 cm in diameter, growing perpendicular to stratification with occasional coated bubbles. It is usually associated with terrigenous and siliciclastic deposits	Lenticular geometries with layers ranging from few tens of decimetres to more than 1 m	Stem coating consisting of homogeneous micrite, clotted micrite and/or microsparite, with peloids, filaments, ostracods and gastropod remains. The reed mould stems mostly remain empty or partly filled by fine sediment or spar crystals	Reed mouldic pores and interparticle pores usually filled by micrite	Marsh environment characterised by reduced influence of thermal water, either cooled down in distal settings away from the vent or mixed with freshwater	Alluvial plain. Particularly occurring in the southern sector of the study area
Peloidal micrite	Wackestone to packstone whitish to beige coloured usually located between clay levels. Gastropods and bioclasts, ostracods and *Charophtye* stems (up to 5 mm long, 0.5 mm in diameter) and intraclasts (up to 1 mm)	Tabular geometries with layers of few decimetres	Wackestone and packstone with amalgamated non-translucent clotted peloidal micrite, intercalated with structureless micrite and microsparite	Low porosity. Vugs	Low-energy environments related to lacustrine-palustrine to stagnant pond or to shallow flat ponds, with occasional terrigenous and freshwater input	Alluvial plain association. Mostly recurrent in the northern and central sectors
Silt with clasts	Grey to dark grey-coloured layers, sometimes finely laminated, with very fine dark detrital siliciclastic silt fraction. Intraclasts, bioclasts and gastropods. Fining-upward trend	Tabular geometries ranging from few decimetres to more than 1 m	—	—	Generally developed at the edges of travertine systems during periods of non-carbonate precipitation. Immature soil deposits sometimes associated with flood events in mudflat areas of alluvial environment	Alluvial plain. Observable in each analysed sector of the study area, but particularly abundant in the southern sector

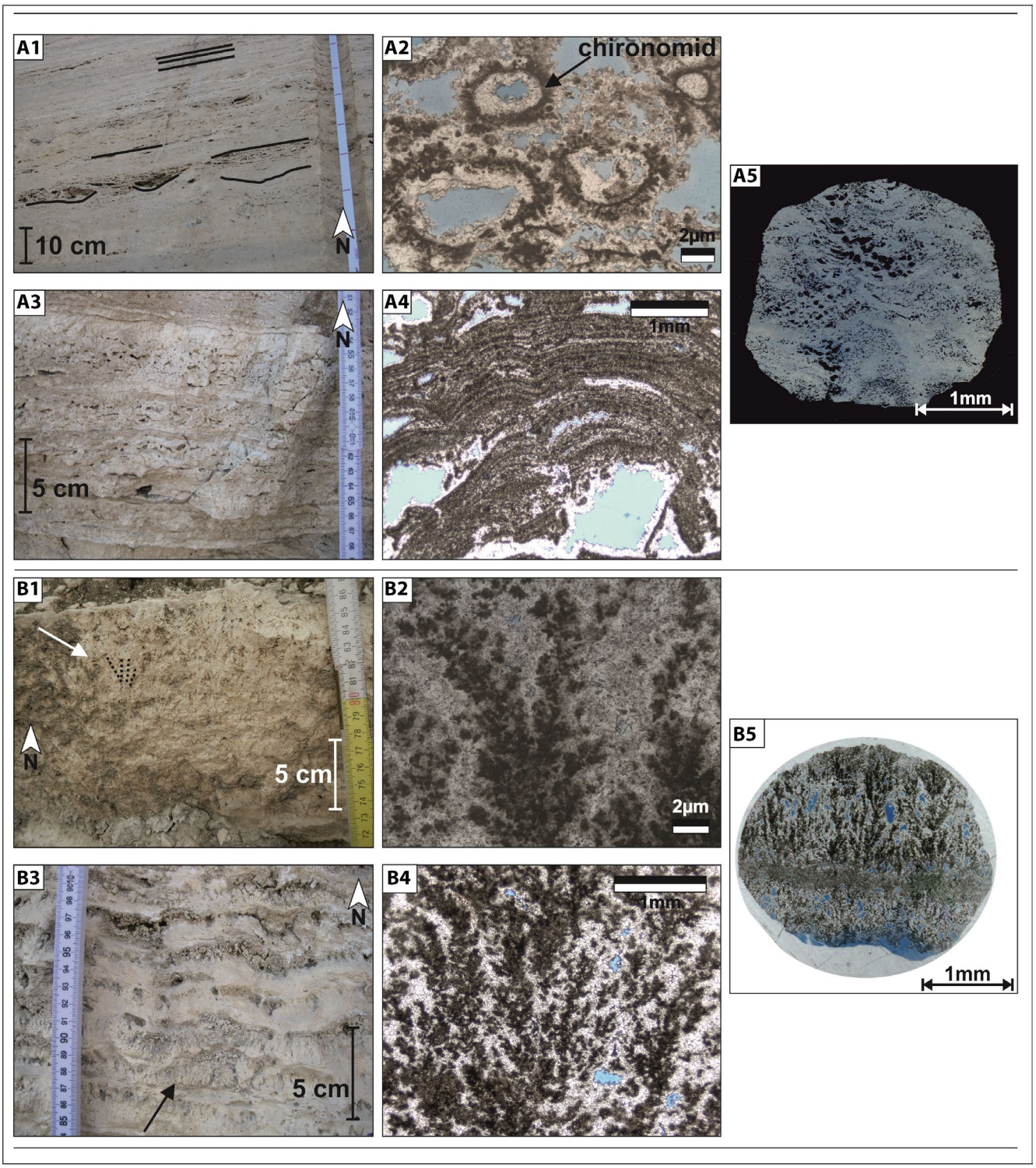

FIGURE 5 Different lithotypes characterising the Testina unit. (A1 and A3) Outcrop view of microbial laminite in QRN quarry; (A2 and A4) Photomicrographs of microbial laminite; (A5) Scanned thin section of microbial laminite; (B1 and B3) Outcrop view of shrub boundstone in QRN quarry; (B2 and B4) Photomicrograph of shrub boundstone; (B5) Scanned thin section of shrub boundstone

Furthermore, the origin of the alternating micritic interlayers within the shrub layers has been interpreted as reflecting the reduced carbonate precipitation during the cold season (Chafetz & Folk, 1984). In agreement with the observations made in active/present-day conditions, bacterial shrubs appear to develop when the water evaporates and the level of the flow drops, while the deposition of lime-mud is a consequence of whitings forming during flooding periods (Erthal et al., 2017; Gandin & Capezzuoli, 2014). Facies similar to the shrub boundstone observed in the Testina are widespread

in hot spring travertines around the world (Chafetz & Folk, 1984; Gandin & Capezzuoli, 2014; Guo & Riding, 1998; Jones et al., 2005; Özkul et al., 2002). Bacterial shrubs are reported from very shallow pools and extensive sheets of still water in waterlogged flats (Chafetz & Folk, 1984; Erthal et al., 2017; Guo & Riding, 1998; Rainey & Jones, 2009). In the Testina, shrub boundstone seems to be related to low-energy environments, originating in thin sheets of thermal waters. In active thermal systems, small clusters of shrubs can be observed developing in several depositional settings, characterised by the rapid evaporation of very thin films of supersaturated waters flowing along sub-vertical walls of semi-dried channels, on the fringe of very shallow slow-running watercourses or within macro and micro-terraces (Gandin & Capezzuoli, 2014).

4.1.3 | Crystalline crust

Description: The crystalline crust lithotype is a cementstone characterised by alternating micrite and sparite laminae (sensu Della Porta, 2015; Della Porta et al., 2017a). Crystalline crust is commonly dense, crudely fibrous with a bright white colour (Figure 6A1, A3). Crusts are made of composite calcite crystals with a feather-like arrangement that developed perpendicularly to the depositional surface. The geometries are tabular and lenticular convex with a thickness from 2 to 3 m with alternating micritic laminae and crystalline crusts. The thickness of the crystalline crust changes from a few millimetres to 5 cm. At a microscopic scale, the crystalline crust lithotype is characterised by intercalations of micrite and sparite (Figure 6A2, A4, A5). Micritic laminae are commonly dark-coloured, whereas sparite laminae are more transparent. Plume-like aggregates can be observed orientated perpendicular to the substrate, progressively shaping some micro-terraces. In thin section it becomes evident that feather crystals are often micritized. Porosity can develop between laminae or between crystals as growth-framework porosity.

Interpretation: The crystalline crust lithotype is linked to a high-energy environment. The feather-like crystalline crusts precipitate directly from very thin sheets of water running on variably steep surfaces, with smooth, laminar flow (Gandin & Capezzuoli, 2008; Guo & Riding, 1998), whereas the alternation of light and dark layers has been interpreted as diurnal variation near spring areas (Guo & Riding, 1998). In the study area, crystalline crusts usually form as sub-horizontal layers, but locally also form undulating structures resembling rims and bumps (Erthal et al., 2017). The crystalline crust cementstone of Testina (sensu Della Porta, 2015) commonly forms as the result of rapid precipitation from fast flowing waters on smooth slopes (Erthal et al., 2017; Okumura et al., 2012).

4.1.4 | Lithoclast travertine

Description: Lithoclast travertine is characterised by packstone to floatstone rich in sub-angular to sub-rounded white coloured clasts with diameters up to 1 cm (Figure 6B1, B3). Lithoclast travertine is typically characterised by sub-horizontal to tabular geometries with layers up to 40 cm thick, beige to dark grey in colour. Microscopic analysis reveals the presence of abundant micrite with peloids and gastropods contained in the matrix around the clasts. This lithotype is characterised by microsparite and elongated bladed (more than 100 μm) to equant or blocky drusy calcite (more than 20 μm) cements, usually strongly micritized. Porosity is associated with vugs located where clast concentrations are highest, although almost completely filled by calcite cement. In contrast, the areas mainly characterised by the presence of micrite show partially cemented pores, usually bordered by bladed cement (Figure 6B2).

Interpretation: Travertine clasts range in shape from spherical to irregularly rounded, depending on water energy. Intra-clasts and extra-clasts, formed by the erosion of the travertine layers located upstream are probably deposited during a pause or diversion of the thermal water input (Della Porta et al., 2017a, 2017b; Erthal et al., 2017; Gandin & Capezzuoli, 2014). The lithoclast travertine composition suggests a distal, palustrine depositional setting in shallow or ephemeral ponds, with clasts derived from the upper part of the slope and including all of the different lithotypes described. Such clasts are subsequently deposited on the lower part of the slope and in depressions, but they could also be locally interpreted as deriving from soft sediment deformation as described by Brogi et al. (2018) in similar depositional environments. Lithoclast travertine of the Testina has a similar macroscale appearance and clast content as comparable facies described by Guo and Riding (1998) in Rapolano Terme (Italy) and interpreted in terms of shallow pools, ponds, micro to macro terrace depositional environments, characterised by low-energy water flows.

4.1.5 | Reed travertine

Description: Reed travertine is characterised by in situ encrusted plant moulds up to 2 cm in diameter, oriented perpendicularly to stratification. Boundstone and sometimes rudstone facies, characterise this lithotype, usually associated with encrusted coated bubbles (Figure 7A1, A2), creating concavo-convex shapes. The thickness of this beige to brownish lithotype ranges from a few tens of decimetres to more than 1 m. It is usually found associated with terrigenous and siliciclastic deposits.

Microscopically, the reed travertine lithotype is characterised by encrusted plant moulds consisting of

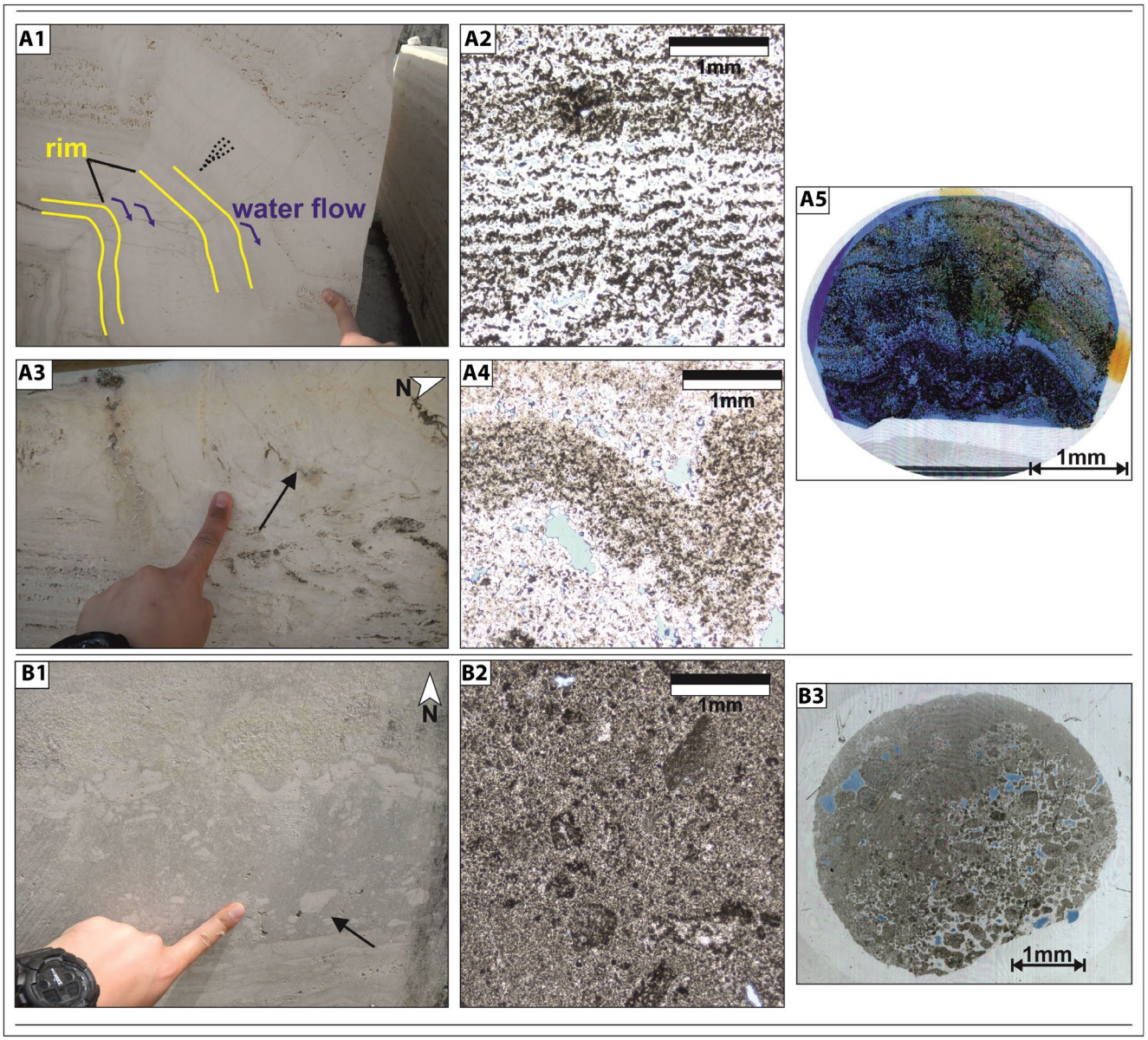

FIGURE 6 Different lithotypes characterising the Testina unit. (A1 and A3) Outcrop view of crystalline crust in GIAN quarry; (A2 and A4) Photomicrograph of crystalline crust; (A5) Scanned thin section of crystalline crust; (B1) Outcrop view of lithoclast travertine in QRN quarry; (B2) Photomicrograph of lithoclast travertine; (B3) Scanned thin section of lithoclast travertine

homogeneous micrite, clotted micrite and/or microsparite, associated with peloids, ostracods and gastropods (Figure 7A3). Porosity is mainly related to reed mouldic pores and to interparticle pores between the plants usually filled by micrite.

Interpretation: Plant moulds, peloids, bioclasts of ostracods and gastropods, are related to the reduced influence of thermal water, either cooled down in distal settings away from the vents or mixed with freshwater, in marsh depositional environments (Capezzuoli et al., 2014; Della Porta et al., 2017a, 2017b; Guo & Riding, 1998; Özkul et al., 2002; Pedley & Rogerson, 2010). Locally, the high density of stems forms barriers to water flow and plants can be encrusted with finely crystalline carbonate deposits (Guo & Riding, 1998). The reed travertine lithotype was previously described by Guo and Riding (1998) in Rapolano Terme (Italy) and subsequently by Özkul et al. (2002) in Denizli (Turkey), while Rainey and Jones (2009) defined it as a macrophyte facies. Higher plant communities grow when the thermal water no longer flows in certain areas. When changes occurred to the water flux or when the water supply was higher, plant stems were submerged by the flowing water and subsequently encrusted by very fast calcium carbonate precipitation, leaving the shape of the plant almost unaltered (Della Porta et al., 2017a, 2017b; Guo & Riding, 1998). The deposition of calcium carbonate around stems is interpreted as a physical

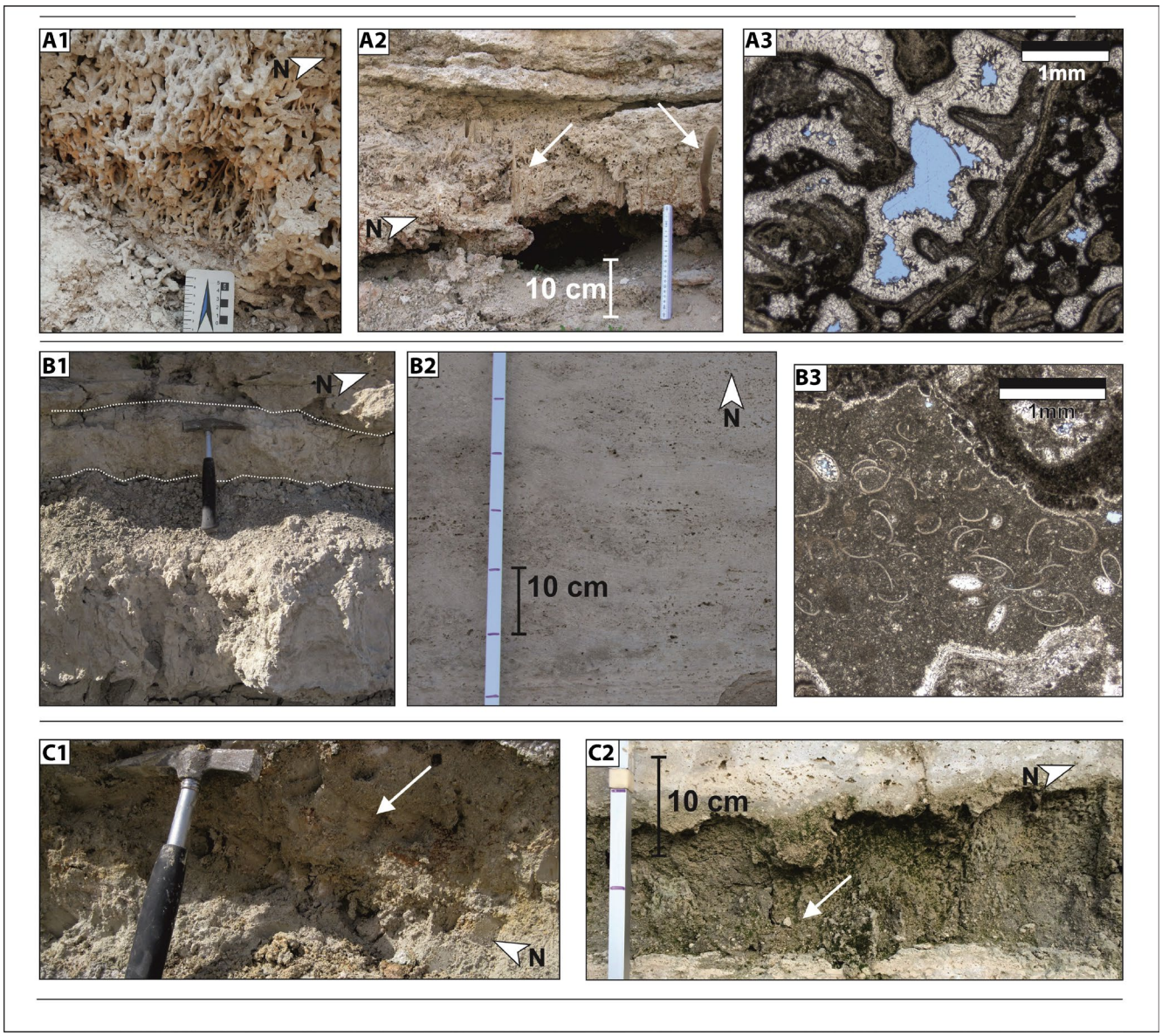

FIGURE 7 Different lithotypes characterising the Testina unit. (A1 and A2) Outcrop view of reed travertine in PACS quarry; (A3) Photomicrograph of reed travertine; (B1 and B2) Outcrop view of peloidal micrite in QRN quarry; (B3) Photomicrograph of peloidal micrite; (C1 and C2) Outcrop view of silt with clasts in PACS quarry

process. Rainey and Jones (2009) suggested that the 'macrophyte facies' is most common at the base of the deposit where local vegetation was inundated by spring water and encrusted with calcite.

4.1.6 | Peloidal micrite

Description: This lithotype displays a wackestone to packstone texture and it is usually located between clay

FIGURE 8 Transmitted light (TL) and cathodoluminescence (CL) images of different lithotypes related to the Testina travertine. (A and B) Microbial laminite lithotype under TL and in CL (A1–B1), characterised by a bright luminescence for micrite and dull luminescence for bladed cement (QRN quarry). (C) Shrub boundstone under TL and in CL (C1), image showing blue to purple dull luminescent clotted micrite within shrub-like structures (QRN quarry). (D) Crystalline crust lithotype under TL and in CL (D1), with fabric of dull luminescent feather-like crystals (GIAN quarry). (E) Peloidal micrite lithotype under TL and in CL (E1), sketch showing a very bright luminescent extra-clast also containing skeletal and gastropods remains (QRN quarry). (F) Lithoclast travertine lithotype under TL and in CL (F1) fabric showing rim cement and a carbonate clast with different cement phases (QRN quarry). (G) Peloidal micrite lithotype under TL and in CL (G1), texture with gastropod filled by non-luminescent blocky cement (PACS quarry). (H) Reed travertine lithotype under TL and in CL (H1), texture showing Chara stem bordered by a thin film of micrite clearly visible in CL (PACS quarry). (I) Lithoclast travertine under TL and in CL (I1), texture of a lime-mud inclusion having the same luminescence as the adjacent blocky cement (QRN quarry)

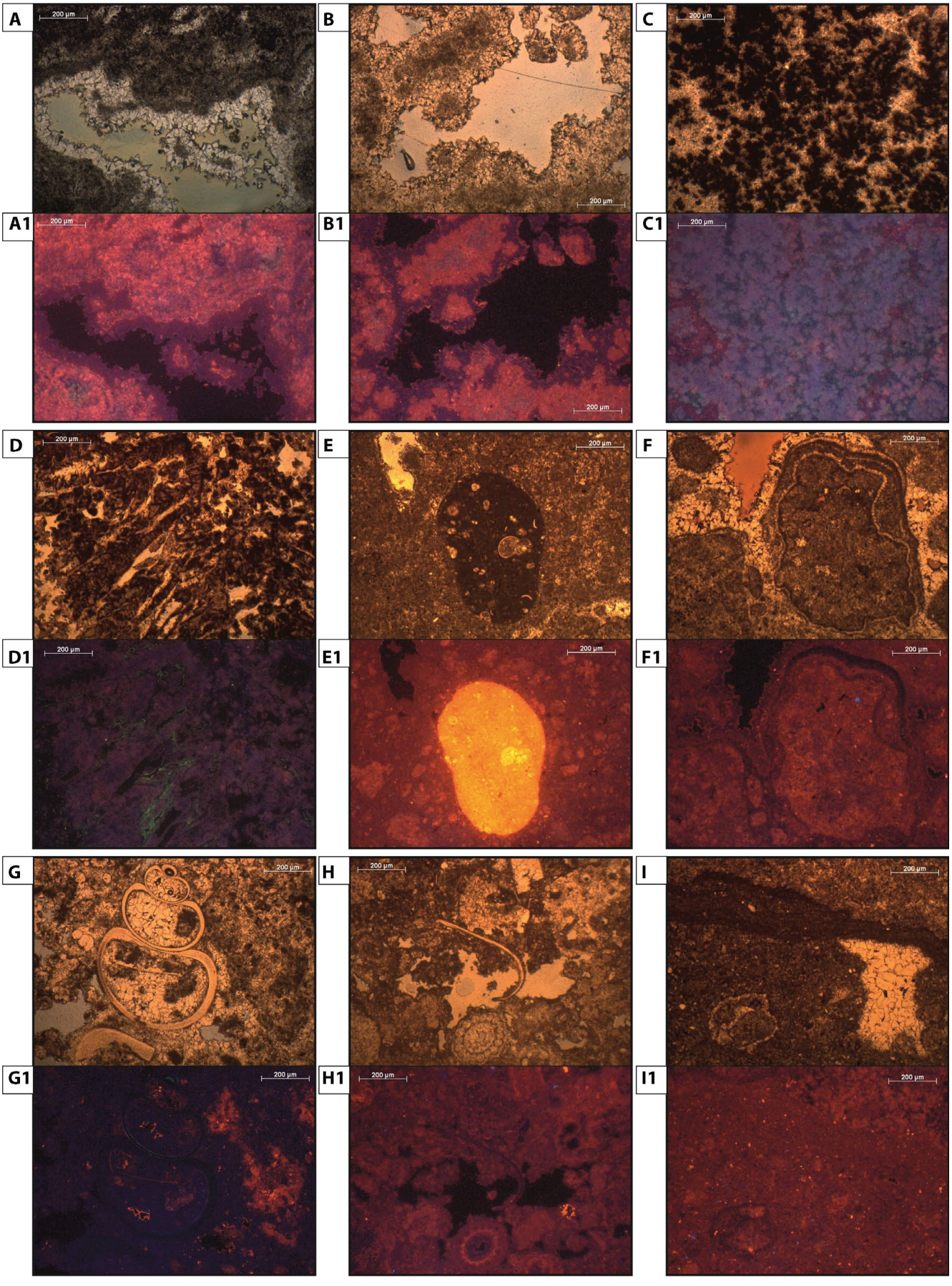

levels, showing a thickness of few decimetres and a whitish to beige colour with tabular geometries (Figure 7B1, B2). Moreover, it also contains gastropods and bioclasts. Microscopically peloidal micrite is characterised by wackestone and packstone with amalgamated non-translucent clotted peloidal micrite, intercalated with structureless micrite and microsparite (Figure 7B3). Gastropods, bioclasts, ostracods, Charophyte stems (up to 5 mm long, 0.5 mm in diameter) and intraclasts (up to 1 mm) frequently occur.

Interpretation: This lithotype is related with lacustrine-palustrine to stagnant pond environments or to shallow flat ponds, with occasional terrigenous and freshwater input, as indicated by the presence of ostracods and Charophytes (Della Porta et al., 2017a; Gandin & Capezzuoli, 2014; Guo & Riding, 1998).

4.1.7 | Silt with clasts

Description: These deposits consist of massive, very fine dark detrital siliciclastic silts that, occasionally, are finely laminated with tabular geometries containing several intraclasts and gastropods (Figure 7C1, C2). The thickness of these grey to dark grey-coloured layers ranges from a few decimetres to more than 1 m. The reworked sediments display a fining upward trend.

Interpretation: This lithotype developed during periods of non-carbonate deposition and/or subaerial exposure (Della Porta et al., 2017a; Erthal et al., 2017) and could be interpreted as soil deposits sometimes associated with flood events in mudflat areas of alluvial environments (Miall, 1996). Neves et al. (2005) interpreted similar lithotypes associated with gravel deposits and developed in lenses, as having formed in ponds with the settlement of fine sediment. The occurrence of gastropods is indicative of fresher and/or cooler waters than those precipitating the travertine facies (Della Porta et al., 2017a; Guo & Riding, 1998). This lithotype is not generally associated with travertine facies, but develops at the edges of travertine systems or during periods of non-carbonate precipitation, representing the most common lateral lithotype of the Testina travertine, which especially occurs in the central and southern part of the study area.

4.2 | Diagenetic features of travertine lithotypes

Cathodoluminescence analysis carried out on Testina lithotypes unravels different diagenetic processes related to (a) cementation, (b) dissolution and (c) sparmicritization (Figures 8 and 9). Calcite cement, characterised by red to purple colours when treated with alizarin varies from microsparite (20 μm) to sparite (50 μm). The reed travertine lithotype shows pendant cements which formed under the downward pull of gravity on water as a result of $CaCO_3$ precipitation from droplets (Alonso-Zarza & Tanner, 2010). Pores are usually almost completely filled by blocky or rim cement and occasionally drusy or bladed cement. In cathodoluminescence, the different lithotypes show alternating bright red to orange zones and dull compositional zones for micrite, whereas the calcite cement usually appears as blue to dark blue dull luminescent (Figure 8A, A1). The micritization process, recognised in all lithotypes, affects calcite cements that appear in cathodoluminescence with a bright red to orange luminescence (Figure 8A, A1, B, B1). In contrast, clotted micrite, usually reflecting microbial activity as, for example, in the shrub boundstone and microbial laminite lithotypes (Erthal et al., 2017), displays a blue to purple dull luminescence (Figure 8B, B1, C, C1). Lithotypes originating from abiotic processes, such as the crystalline crust, are also characterised by a blue to dark blue dull luminescence (Figure 8D, D1). Extra-clasts observed in cathodoluminescence, possess bright luminescence compared to their surrounding micrite (Figure 8E, E1), while intraclasts of lithoclast travertine and microbial laminite lithotypes, are characterised by multiple phases of bright and dull luminescence (Figure 8F, F1). Bioclasts and plant moulds in cathodoluminescence (Figure 8G, G1) are non-luminescent. Dull luminescence instead is observed when micritization phenomena occurs (i.e. Charophytes stems; Figure 8H, H1). The lime-mud layers, mainly characterising lithotypes such as microbial laminite and lithoclast travertine, possess the same dull luminescence as calcite cements, revealing that they belong to the same stage of diagenesis (Figure 8I, I1). The Testina travertine appears as a poorly lithified deposit but unexpectedly shows a high degree of cementation, in particular those lithotypes occurring in the northernmost quarry (QRN quarry). Proceeding southward to the GIAN and PACS quarries, cementation becomes gradually less common and travertine pores are usually open due to meso-scale to micro-scale dissolution process.

4.3 | Vertical and horizontal organisation of Testina geobodies

The intensive travertine quarrying activity that occurred in the Acque Albule Basin over the past few decades allows for observation and correlation of vertical and horizontal variations of individual geobodies (Figures 10–12). The different geobodies characterising the entire Testina were divided, based on bounding discontinuities observable and mappable at sub-basin scale. The recognised discontinuities are mainly related to erosion and non-deposition, defining six different geobodies. The lowermost surface, differentiating the Testina travertine from the *Lapis Tiburtinus* travertine, corresponds

with the S1 surface described by Faccenna et al. (2008). In the northern part of the study area, the surfaces are covered by the lithoclast lithotype in the lower part of the study succession, while in the upper part the lithotype is made up of thin layers of brown to grey silt with clasts. In the central part, these surfaces locally show erosional characteristics, covered by the peloidal lithotype. In the southern part of the study area, unconformity surfaces are discontinuous and lenticular, covered by grey-brown silt with clast and lithoclast travertine lithotypes.

The QRN quarry (Figure 10), located to the north of the study area, displays geobodies mainly composed of microbial laminite, associated with shrub boundstone and interbedded with lithoclast travertine and, occasionally, crystalline crust lithotypes (Geobodies 1, 2 and 3). The upper part of the investigated succession is characterised by detrital silt with clasts of Geobody 4, followed by crystalline crust pertaining to Geobody 5. Geobody 6 is instead mainly composed of the reed travertine lithotype. The different identified geobodies (Figure 10 A1, A2) have subhorizontal bedding with an inclination of 20° toward the east. The geobodies in GIAN quarry (Figure 11), located in the central part of the study area, are marked by shrub boundstone interbedded with microbial laminite and peloidal micrite in centimetre-thick layers (Gebodies 1–5). An erosional surface divides Geobody 5 from Geobody 6. This latter geobody is dominated by the crystalline crust lithotype (Figure 11 A1, A2), locally with strongly undulated geometries when compared with Geobodies 1–5, characterised instead by tabular geometries. Located in the southern part of the study area, the PACS quarry (Figure 12A) shows the predominance of microbial laminite in Geobody 1 passing upward to the crystalline crust lithotype of Geobody 2, forming undulated layers and pinch-out structures. Geobody 3 instead, is composed of silt with clasts passing upward to the reed lithotype. Geobody 4 is composed of the microbial laminate lithotype, passing to reed travertine more than 1 m thick and related to Geobody 5, characterised by an erosional surface at the top. Geobody 6 developed on top of the erosional surface and is characterised by the crystalline crust lithotype and layers of microbial laminites lithotype, sometimes associated with carbonate clasts. The overall geobodies described have principally sub-horizontal bedding (Figure 12 A1, A2, A3).

5 | DISCUSSION

5.1 | Controlling factors on Testina travertine depositional system

The interpretation of the depositional environments of the Testina travertine was delineated based on the identification of physical (grain size, components, erosional features and bedding), chemical (inorganic, dissolution and precipitate) and biological processes (Brasier, 2011; Toker et al., 2015; Török et al., 2017) affecting the different lithotypes.

The six geobodies composing the Testina travertine have lithotype associations attesting to different energetic conditions, gradually changing from north toward south over the study area. Based on lithotype interpretations and spatial distribution, the seven different lithotypes previously described (see Section 4.1 and Table 1) are attributed to three different depositional settings: (a) shallow lake, (b) slope and (c) alluvial plain.

The northernmost QRN quarry, mostly characterised by microbial laminite and shrub boundstone lithotypes, identified this part as the most proximal area within the basin, characterised by a shallow lake (Figure 13A). The abundant presence of these lithotypes indicates an environment characterised by low water energy conditions (Guo & Riding, 1998) (Figure 13B,C; Geobodies 1–4). Silty levels recognised in the upper part of the logged section highlight the reduced or interrupted carbonate deposition (see log 1a and 1b in Figure 13A,C; Geobody 5). Subsequently, the carbonate system returns to its previous situation, depositing crystalline

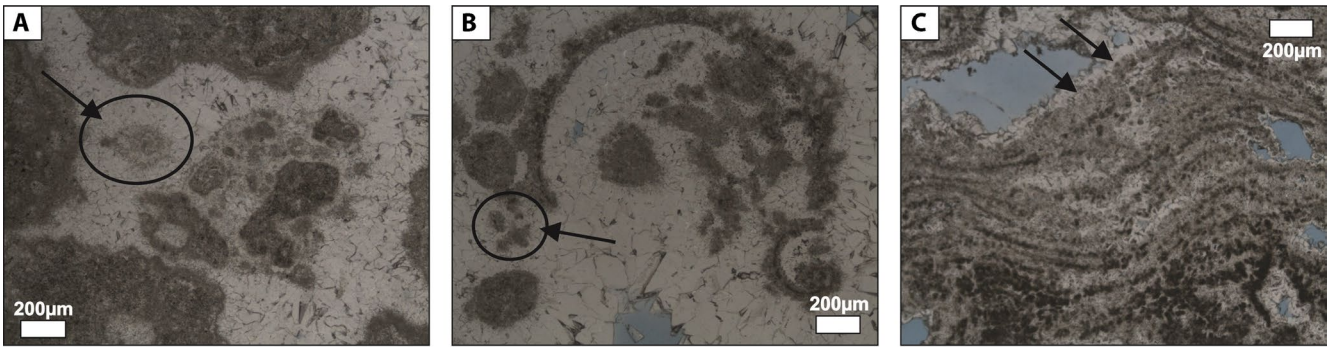

FIGURE 9 Examples of sparmicritization affecting the crystalline crust and microbial laminite lithotypes. (A and B) In the crystalline crust the sparite is replaced by micrite generally with a sub-rounded shape. (C) In the microbial laminite boundstone the process instead affects the sparitic laminae

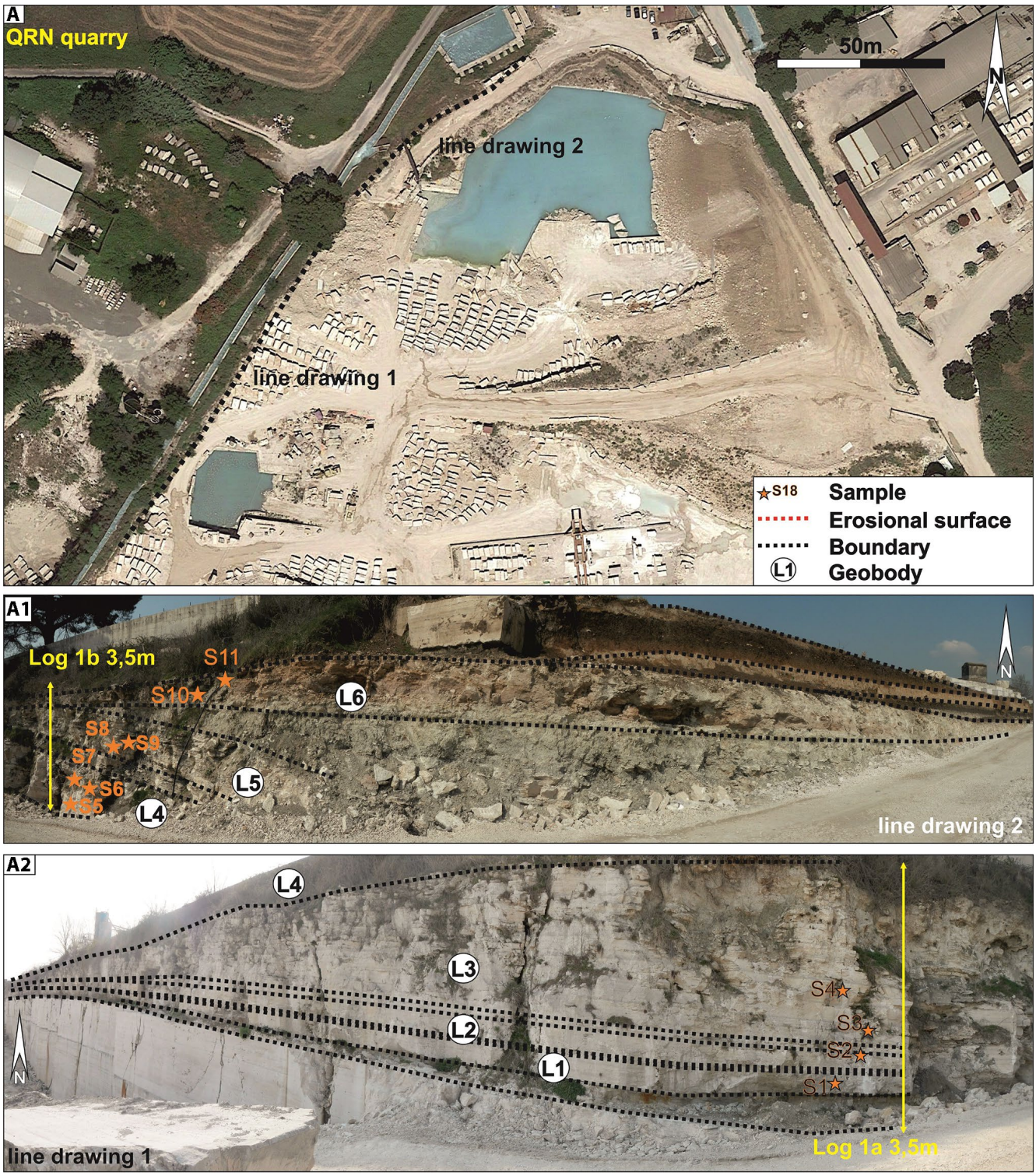

FIGURE 10 (A) Map of QRN quarry (northern part of the study area). (A1–A2) Line drawing and positions of the stratigraphic logs and samples collected (partially modified from Google Earth, Digital Globe, 2020)

crust and reed travertine lithotypes, suggesting the presence of a slope depositional environment prograding towards the south (Figure 13A–C; Geobody 6) and representing the last depositional event of the Testina travertine.

The GIAN quarry, located in the central part of the study area, is characterised by prevalent horizontal geobodies composed of shrub boundstone and microbial laminate, indicating a shallow lake depositional environment, passing subsequently into an erosional surface to smooth slope lithotype (crystalline crust; Della Porta et al., 2017a; Guo & Riding, 1999). Thus, it can be identified as deposited in a more

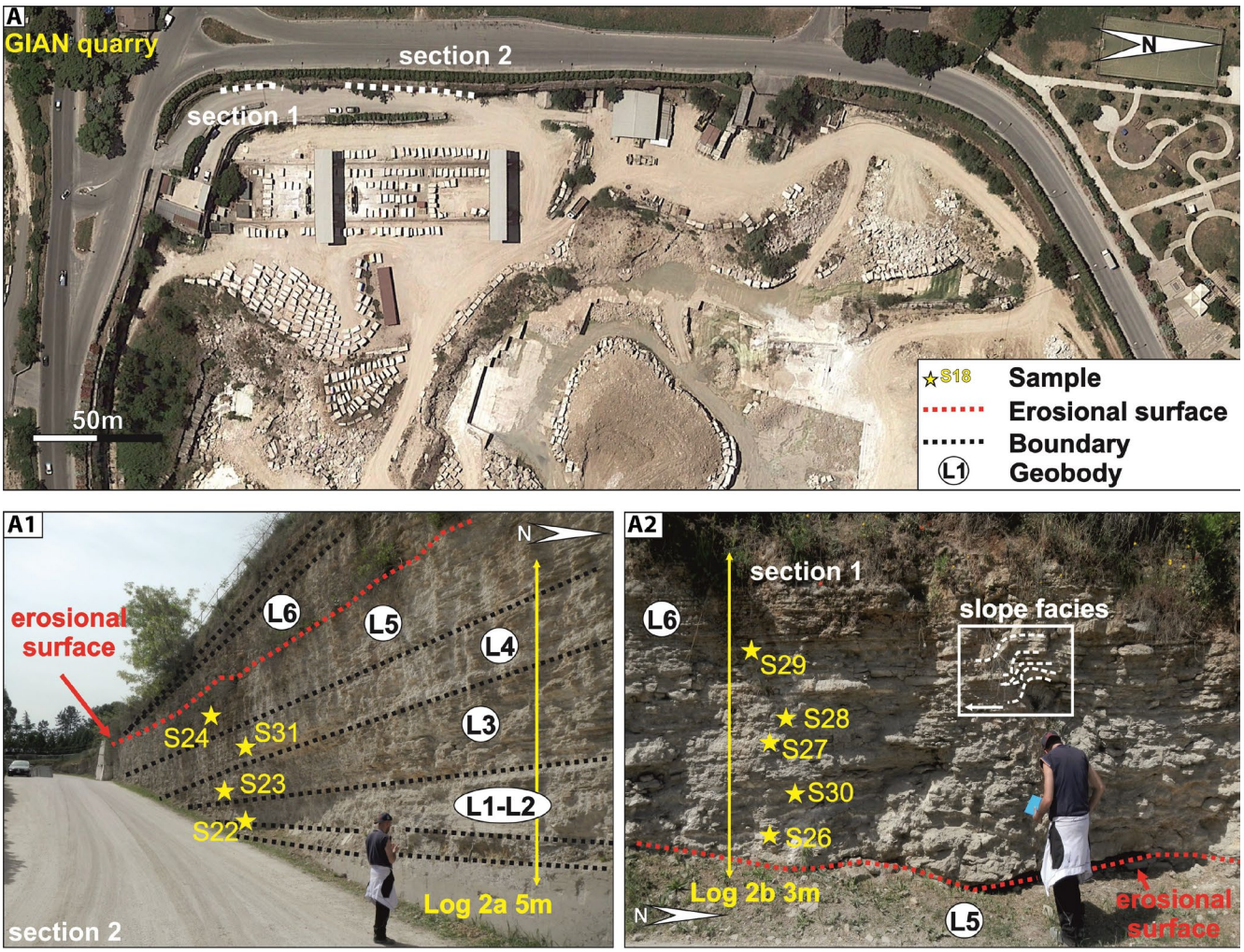

FIGURE 11 (A) Map of GIAN quarry (central part of the study area). (A1–A2) Line drawing and positions of the stratigraphic logs and samples collected (partially modified from Google Earth, Digital Globe, 2020)

distal setting with respect to the main thermal water spring (Figure 13A–C).

The PACS quarry, situated in the southernmost part of the study area, is characterised by microbial laminite, crystalline crust and reed travertine interbedded with alluvial siliciclastic deposits related to the silt with clasts lithotype (Figure 13A), suggesting that this part of the depositional system corresponded to a distal zone, with environmental conditions similar to an alluvial plain (Figure 13B,C; Geobodies 1–5). Flooding events due to seasonal variations or climate changes related to the nearby Aniene River could be responsible for such interbedding of travertine with the alluvial deposits. In the Acque Albule Basin, the combination of gently dipping topography (3°–4°; Della Porta et al., 2017a; Erthal et al., 2017; Mancini et al., 2019a) from north toward south, spring-water supply and mixing with meteoric cool-water created a complex interplay between low-energy subaqueous and high-energy slope lithotypes which constitute the Testina geobodies. The general trend displayed by the Testina geobodies consists of alternating slope and shallow lake lithotype associations, characterising the north and the central part of the study area. In addition to the latter lithotype association, the southern sector of the study area shows the widespread presence of the silt with clasts lithotype, pertaining to an alluvial plain setting. The Testina geobodies are mainly characterised by aggradational and progradational patterns toward the south. The sub-horizontal layering, typical of shallow lake deposits, sometimes is interrupted by undulated lithotypes representing smooth slope deposits, or by erosional surfaces occurring when the whole spring-water outflow is strongly decreased, ceased or changed (as also described in the lower travertine succession of the *Lapis Tiburtinus* travertine; Della Porta et al., 2017a; Erthal et al., 2017). Such sub-horizontal bedding is commonly cyclic due to the alternation of dominantly biotic and abiotic fabrics. Cyclicity reflects changes in the physico-chemical variables of the water related mainly to changes in the water supply and the consequent energy of the water flow (Della Porta et al., 2017a; Erthal et al., 2017). The vertical change from flat to gently

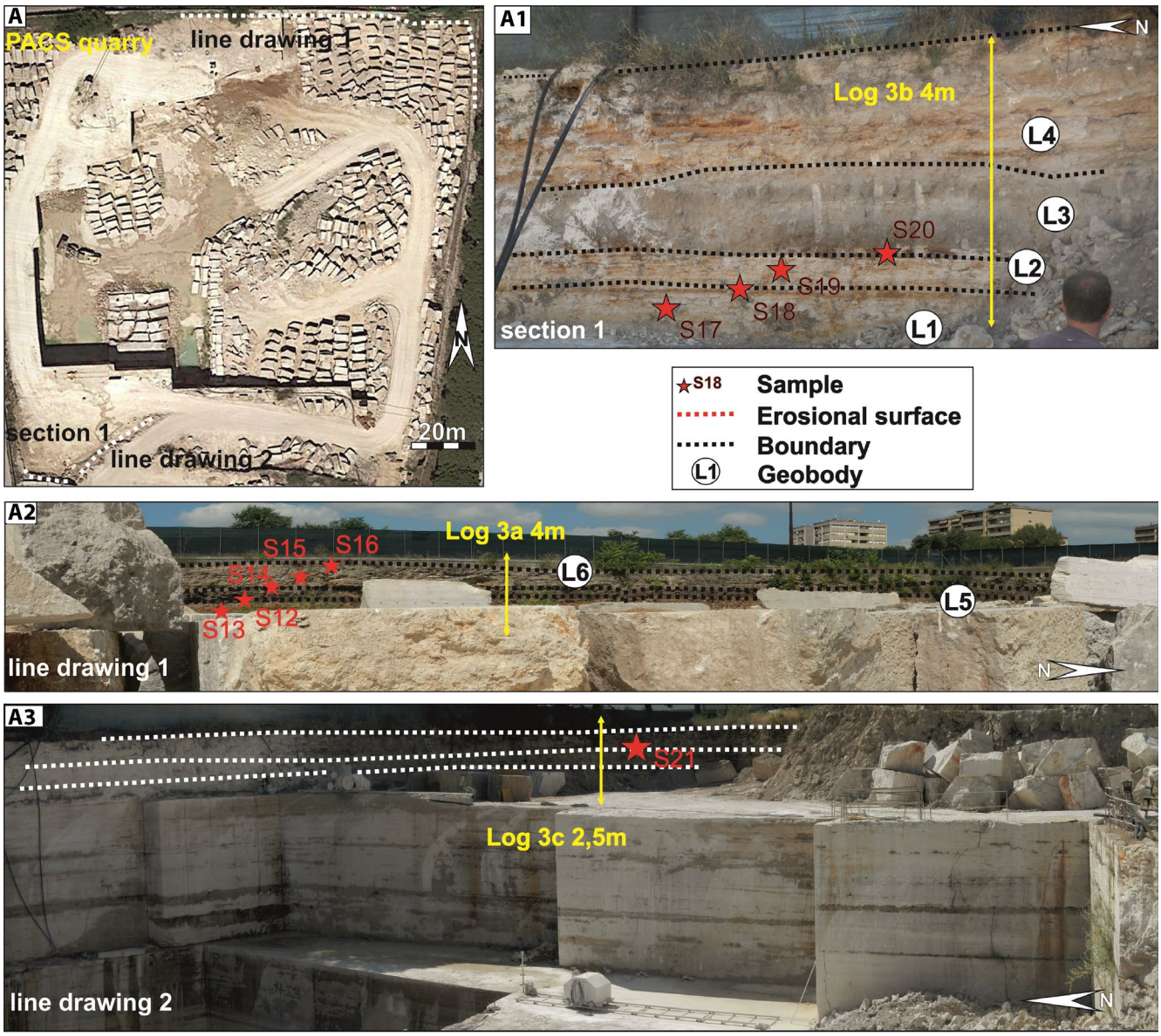

FIGURE 12 (A) Map of PACS quarry (southern part of the study area). (A1–A2–A3) Line drawing and positions of the stratigraphic logs and samples collected (partially modified from Google Earth, Digital Globe, 2020)

dipping lithotypes results in undulating layers, reflecting a more complex topography that causes rapid carbonate precipitation. Due to an increase in flow rates, or spring migration, proximal or distal depression environments could be invaded by higher energy flowing water resulting in progressively enhanced precipitation of crystalline crusts rather than sub-horizontal pool and marsh travertines, as also suggested by Della Porta et al. (2017a) in their study regarding the well-lithified *Lapis Tiburtinus*. Vertical lithotype transitions are very sharp, suggesting that spring water flow rates varied greatly and fluctuated often in response to factors other than topography, such as flow re-direction from the springs or changes in the volume of water discharged from the vent (Della Porta et al., 2017a). Flow re-direction may account for localised lithotype changes, but only discharge volume changes could have affected widespread lithotype development concurrently at proximal and distal parts of the depositional system (Mancini et al., 2019a).

The boundary between the marsh-pool and the smooth slope lithotypes, in vertical section, is generally marked by an erosional surface (Guo & Riding, 1998). Erosional horizons are related to periods with low or no-spring water discharge, which leads to subaerial exposure of the previously deposited travertines. An erosional phase is usually coincident with a change in the depositional environment and, thus, in the lithotype too. This is clear in the GIAN quarry, where the erosional surface marks the transition between the flat-pool facies and the overlying lithotypes, which are characterised by crystalline crust with undulated structures related to an inclined morphology. This erosive surface is probably related

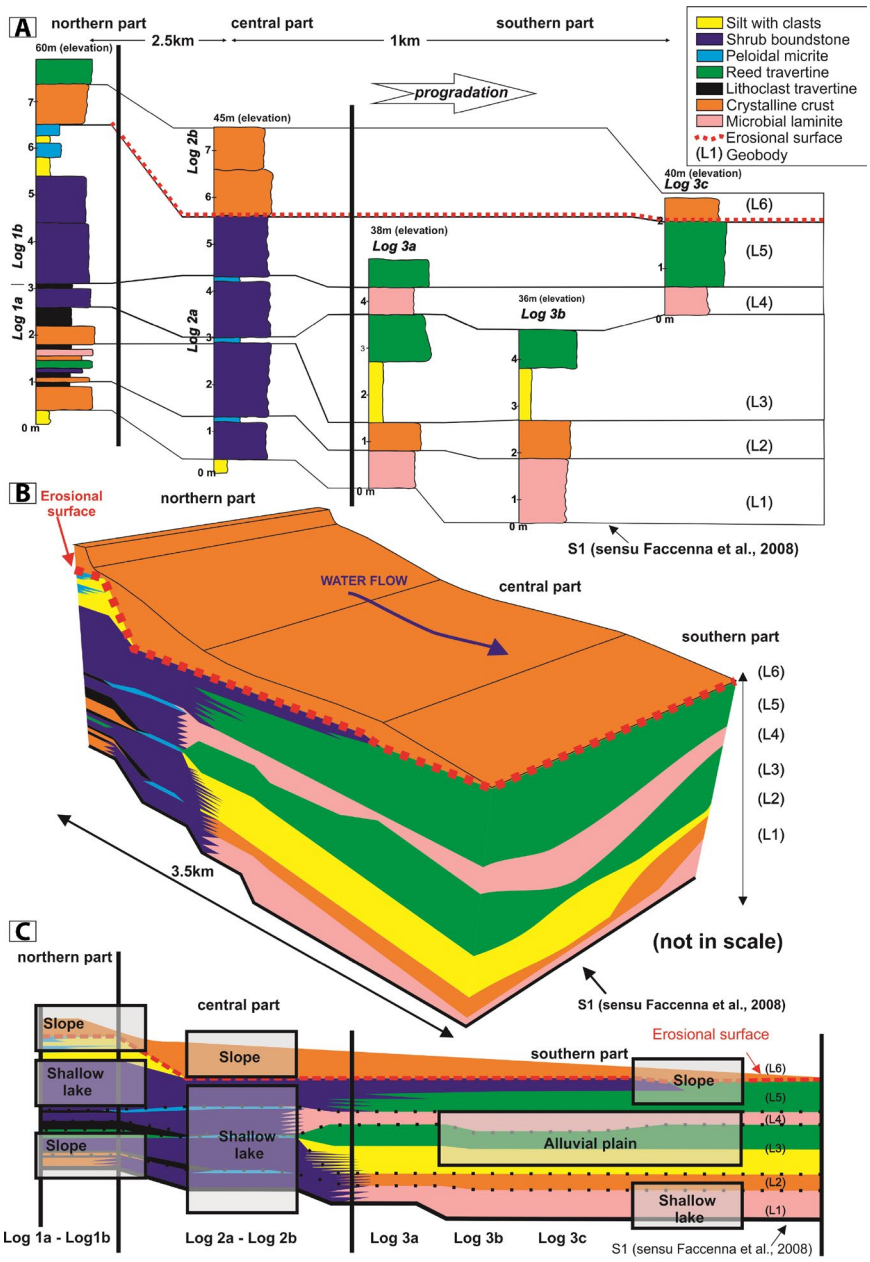

FIGURE 13 (A) Overview of stratigraphic logs. (B) 3D model reconstruction, based on the correlation between the different geobodies. (C) Correlation panel of the different Testina travertine geobodies recognised in the study area, with each depositional environment defined on the basis of lithotype association. Geobody 1 lithotype association indicates high-energy environmental conditions in the north, which passes gradually to a low-energy environment towards the south. Geobody 2 and 3 lithotype associations indicate high-energy environmental conditions in the north, passing to low-energy environmental conditions in the central part and high-energy conditions in the south. Geobody 4 and 5 displays lithotype associations related to homogeneous environmental conditions in all analysed sections, pertaining to low-energy settings. Geobody 6, representing the last depositional stage of the Testina travertine, is mainly characterised by a lithotype association attributed to a high-energy environment

to the lowering of the water table (De Filippis et al., 2013b). According to Faccenna et al. (2008) and De Filippis et al. (2013a) the evolution of the Acque Albule Basin and the entire *Lapis Tiburtinus* travertine succession was controlled by tectonic activity and climate variations as also reported by Anzalone et al. (2017). Discontinuities and fracture distribution controlled the upwelling of high temperature fluids rich in CO_2, that finally mixed with the shallow water aquifer (Carucci et al., 2012; De Filippis et al., 2013a; Della Porta et al., 2017a; Mancini et al., 2019a; Minissale et al., 2002). The climate changes affecting the Late Pleistocene, controlled the elevation of the water table and finally the water discharged by the springs (Della Porta et al., 2017a; Faccenna et al., 2008).

This study suggests that the Testina travertine depositional system was affected and controlled by these factors in different ways depending on the geographic positions. The position of the active vents and their location have particularly influenced the deposition in the northern part, with only local crisis of carbonate deposition mainly related to changes in the direction of the water flow. The central part, however, seems more influenced by the topographic gradient and the water discharge, as also reported by Della Porta et al. (2017a). The southern sector, corresponding to the distal part of the Testina depositional setting, seems more influenced by flooding events related to the Aniene River than tectonic activity, with travertine deposits less cemented due to the mixing of thermal water with freshwater.

Tectonic activity, controlling the position of the springs, has had more influence on the northern part of the study area while flood events of the Aniene River, related to climate fluctuations or seasonal changes, are able to affect the development of the Testina travertine in the southern part.

5.2 | The effect of diagenetic overprinting

The diagenetic history of the Testina travertine can be linked, as also reported by Della Porta et al. (2017a) for the *Lapis Tiburtinus* travertine, to the interaction of the semi-confined aquifer, rainfall precipitation and surficial drainage. The type of cements observed in the Testina travertine lithotype and filling the porosity are principally related to vadose and phreatic meteoric precipitation. This conclusion is supported by the cathodoluminescence, where luminescence indicates growth phases related to reducing conditions indicating phreatic water circulation.

As reported by De Boever et al. (2017a), the open pore systems of travertine deposits have probably led to a high initial water–rock interaction and fast saturation of the infiltrating fluids. In this view, fluids causing cementation in the Testina travertine originated from thermal water and meteoric water or by a mixture (Della Porta et al., 2017a). Water is able to flow through the empty pores and the lower flow velocity could influence the precipitation of calcite cements.

The petrographic analyses performed suggest a main composition of almost pure $CaCO_3$ based on alizarin staining that occurs mostly as calcite. The Testina travertine is poorly lithified (see Figure 7A1, A2 and Figure 12 A1) and is sometimes un-cohesive, although with an unexpectedly high degree of cementation in the northernmost quarry (QRN quarry), while it becomes less cemented toward the southern sector in the GIAN and PACS quarries, where pores usually remain empty.

Decimetre to millimetre sized dissolution vugs are widespread and usually partially or totally filled by blocky or isopachous cements. Such a process reveals that the Testina travertine deposits were frequently affected by periods of non-deposition, during which meteoric diagenesis, caused by flowing of undersaturated water, strongly influenced the final fabric. Sparmicritization processes involving the transformation of calcite spar crystals into micrite is a typical early diagenetic effect induced by bacterial processes (Alonso-Zarza & Tanner, 2010) and characterised by concomitant dissolution and precipitation of calcite particles (Guo & Riding, 1992, 1994; Török et al., 2017). Such a process frequently affects lithotypes such as microbial laminites and crystalline crusts (see Figure 9A–C). In the Testina lithotypes, sparmicritization generally occurs after, or at the same time as, the dissolution process, originating in a fraction of micrite inside crystals of sparry calcite. Loose clay and silt-sized grains of calcite could be produced during sparmicritization associated with water table fluctuations. Such particles can form vadose silt that contributes to the internal sediment, which may be deposited in available pores (Chilingarian & Wolf, 1994). In contrast, the clotted peloidal micrite in the Testina lithotypes is not derived from micritization processes but is a primary deposit. These differences are highlighted by cathodoluminescence analyses in which a distinct dull luminescence is identified for the clotted peloidal micrite, while a bright luminescence is emitted by the micritized fraction.

In this view, groundwater composition in the northern area was characterised by higher rates of supersaturation with respect to calcium carbonate, due to spring proximity, and decreasing in the southern area due to the dilution of groundwater with meteoric water. The CO_2 degassing and the rapid carbonate precipitation due to the water flowing downstream represent the most important factors able to influence carbonate precipitation as also reported for the underlying *Lapis Tiburtinus* travertine deposits (Della Porta et al., 2017a; Mancini et al., 2019b). Another possible explanation for these differences lies in the topographic gradient, allowing groundwater a higher residence time, thus enhancing cementation of the lithotypes located in the northernmost area. Furthermore, the central part shows units characterised by slightly steeper geometries, which allowed an easier water flow toward the Aniene River. In addition to the limited time for the cementation process to take place, considering the Late Pleistocene–Holocene age of this deposit, this resulted in reduced cementation.

5.3 | Testina travertine as a possible subsurface analogue

The sedimentological analyses and the geobody reconstructions integrated with diagenetic observations allow the reconstruction of factors influencing the different depositional settings. Furthermore, the spatial distribution of some lithotypes allows for better definition of some geobodies in the case of subsurface reservoir analogues. In this view, the presence of travertine deposits in the Brazilian and Angolan Pre-salt is reported by many authors (Renaut et al., 2013; Sabato Ceraldi & Green, 2016; Saller et al., 2016; Wright & Barnett, 2015), as well as the presence of shrub-like fabrics, considered to be one of the most promising reservoir units (Alvarenga et al., 2016; Dias, 2004; Rezende & Pope, 2015; Saller et al., 2016; Wright, 2012; Wright & Barnett, 2015). Despite the difference between the Pre-salt shrubs, principally composed of crystalline fabrics, the shrub boundstone of the Testina travertine could represent an important analogue in terms of depositional setting and environmental conditions, principally related to a supersaturated environment affected by high carbonate precipitation and evaporation phenomena (Basso et al., 2020; Erthal et al., 2017).

Shrub boundstone occurrences are reported by many authors from several places in the world (Japan, Turkey, Italy, USA; Chafetz & Folk, 1984; Della Porta et al., 2017a, 2017b; Erthal et al., 2017; Fouke, 2011; Fouke et al., 2000; Guo & Riding, 1994, 1998; Kitano, 1963), forming in chemically harsh and hot hydrothermal waters, in shallow lakes and depressional depositional settings or in flat waterlogged environments (Chafetz & Folk, 1984; Chafetz & Guidry, 1999; Capezzuoli et al., 2014; Claes et al., 2017b; Erthal et al., 2017; Guo & Riding, 1998; Jones & Renaut, 1995; Jones et al., 2000; Turner & Jones, 2005). The study of the Testina shrub boundstone shows that such lithotypes can be associated with kilometre-scale depositional environments, as in the case of the shallow lake described in the Testina travertine, laterally passing to an alluvial plain and interdigitating with siliciclastic deposits.

In this view, the result obtained by this study permits better definition of the possible geometries that can be observed in subsurface analogues. The Angolan Pre-salt geometries reported in seismic lines are similar to a local lacustrine carbonate platform that, based on data presented here, can be interpreted as a travertine tabular distal body, related to a shallow lake system passing laterally into an alluvial plain (Alvarenga et al., 2016).

6 | CONCLUSIONS

The Testina travertine, representing the last depositional stage of the *Lapis Tiburtinus* travertine is characterised by a depositional system influenced by tectonic activity, topographic gradient, water discharge and flood events related to the Aniene River. This study reveals the importance of such features in the travertine depositional system as well as the possibility to understand the role of these factors in different locations. Furthermore, the Testina travertine, neglected until now by the several studies performed in the Acque Albule Basin and considered to be non-lithified travertine, shows a high degree of cementation particularly in the northern sector, probably related to the composition and/or residence time of the groundwater during deposition. Moreover, based on geometries, lithotype distributions and architecture of the different geobodies, it becomes clear how shrub boundstone units in particular can be characterised by their kilometre-scale distribution. These results could be useful in the interpretation of subsurface reservoir units as in the case of the Brazilian and Angolan Pre-salt subsurface deposits.

ACKNOWLEDGEMENTS

A special thank you goes to Shell, Total and Petrobras for their support of the TraRas project and to the quarry owners (Alessandro, Francesco, Maurizio, Francesca, Aurelio and Roberto of Querciolaie-Rinascente, Giansanti and Pacifici quarries), who granted the possibility to access the quarries and for their logistic support. I warmly thank everyone of the department of Earth and Environmental Sciences (Division of Geology) of the KU Leuven University for their collaboration. Thanks to their facilities it was possible to realize this study. In particular, I am very grateful to Jeroen Soete, Marcelle Erthal, Cihan Aratman, Wim Vandewijngaerde, Zahra Mohammadi, Agnes Torok, Nick Janssens and Robin Honlet, for their friendships and the fundamental contribution they gave to this project during my Erasmus traineeship in Belgium. Herman Nys is thanked for producing high quality thin-sections. The editor, Giovanna Della Porta, is warmly acknowledged. A. Brogi, M. Cihat Alçiçek and two anonymous reviewers are thanked for their helpful comments that have improved the quality of the manuscript.

DATA AVAILABILITY STATEMENT

The data that support the findings of this study are available from the corresponding author upon reasonable request.

ORCID

Fabio Scalera https://orcid.org/0000-0002-2214-5433
Enrico Capezzuoli https://orcid.org/0000-0002-4199-1870
Hannes Claes https://orcid.org/0000-0002-2424-6975

REFERENCES

Acocella, V. & Funiciello, R. (2006) Transverse systems along the extensional Tyrrhenian margin of Central Italy and their influence on volcanism. *Tectonics*, *25*(2), 1–24.

Alonso-Zarza, A.M. & Tanner, L.H. (2010). *Carbonates in continental settings: geochemistry, diagenesis and applications*, vol. *61*. Developments in Sedimentology. Amsterdam: Elsevier.

Alvarenga, R.S., Iacopini, D., Kuchle, J., Scherer, C.M.S. & Goldberg, K. (2016) Seismic characteristics and distribution of hydrothermal vent complexes in the Cretaceous offshore rift section of the Campos Basin, offshore Brazil. *Marine and Petroleum Geology*, *74*, 12–25.

Anzalone, E., D'Argenio, B. & Ferreri, V. (2017) Depositional trends of travertines in the type area of Tivoli (Italy). *Rendiconti Lincei*, *28*(2), 341–361.

Aratman, C., Özkul, M., Swennen, R., Hollis, C., Marques Erthal, M., Claes, H. & Mohammadi, Z. (2020) The giant Quaternary Ballık travertine system in the Denizli Basin (SW Turkey): a palaeoenvironmental analysis. *Quaternaire. Revue de l'Association française pour l'étude du Quaternaire*, *31*(2), 91–116.

Basso, M., Belila, A.M.P., Chinelatto, G.F., da Ponte Souza, J.P. & Vidal, A.C. (2020) Sedimentology and petrophysical analysis of pre-salt lacustrine carbonate reservoir from the Santos Basin, southeast Brazil. *International Journal of Earth Sciences*, 1–23.

Billi, A. & Tiberti, M.M. (2009) Possible causes of arc development in the Apennines, central Italy. *Geological Society of America*, *121*(9–10), 1409–1420.

Billi, A., Tiberti, M.M., Cavinato, G.P., Cosentino, D., Di Luzio, E., Keller, J.V.A., Kluth, C., Orlando, L., Parotto, M., Praturlon, A., Romanelli, M., Storti, F. & Wardell, N. (2006) First results from

the CROP-11 deep seismic profile, Central Apennines, Italy: evidence of mid-crustal folding. *Journal of Geological Society London*, *163*(4), 583–586.

Billi, A., Valle, A., Brilli, M., Faccenna, C. & Funiciello, R. (2007) Fracture-controlled fluid circulation and dissolution weathering in sinkhole-prone carbonate rocks from Central Italy. *Journal of Structural Geology*, *29*(3), 385–395.

Bosence, D., Gibbons, K., Le Heron, D.P., Morgan, W.A., Pritchard, T. & Vining, B.A. (2015) Microbial carbonates in space and time: introduction. *Geological Society of London, Special Publications*, *418*, 1–15.

Brasier, A.T. (2011) Searching for travertines, calcretes and speleothems in deep time: processes, appearances, predictions and the impact of plants. *Earth-Science Reviews*, *104*(4), 213–239.

Brogi, A. (2004) Faults linkage, damage rocks and hydrothermal fluid circulation: tectonic interpretation of the Rapolano Terme travertines (southern Tuscany, Italy) in the context of Northern Apennines Neogene-Quaternary extension. *Eclogae Geologicae Helvetiae*, *97*(3), 307–320.

Brogi, A., Alçiçek, C.M., Yalçiner, C.C., Capezzuoli, E., Liotta, D., Meccheri, M., Rimondi, V., Ruggieri, G., Gandin, A., Boschi, C., Büyüksaraç, A., Alçiçek, H., Bülbül, A., Baykara, M.O. & Shen, C.C. (2016) Hydrothermal fluids circulation and travertine deposition in an active tectonic setting: insights from the Kamara geothermal area (western Anatolia, Turkey). *Tectonophysics*, *680*, 211–232.

Brogi, A., Capezzuoli, E., Alçiçek, M.A. & Gandin, A. (2014) Evolution of a fault-controlled fissure-ridge type travertine deposit in the western Anatolia extensional province: the Çukurbağ fissure-ridge (Pamukkale, Turkey). *Journal of the Geological Society*, *171*, 425–441.

Brogi, A., Capezzuoli, E., Buracchi, E. & Branca, M. (2012) Tectonic control on travertine and calcareous tufa deposition in a low-temperature geothermal system (Sarteano, Central Italy). *Journal of the Geological Society of London*, *169*(4), 461–476.

Brogi, A., Capezzuoli, E., Moretti, M., Olvera-García, E., Matera, P.F., Garduno-Monroy, V. & Mancini, A. (2018) Earthquake-triggered soft-sediment deformation structures (seismites) in travertine deposits. *Tectonophysics*, *745*, 349–365.

Brogi, A., Lazzarotto, A., Liotta, D. & Ranalli, G. (2005) Crustal structures in the geothermal areas of southern Tuscany (Italy): insights from the CROP 18 deep seismic reflection lines. *Journal of Volcanology and Geothermal Research*, *148*(1–2), 60–80.

Brogi, A., Liotta, D., Capezzuoli, E., Matera, P.F., Kele, S., Soligo, M., Tuccimei, P., Ruggieri, G., Yu, T.L., Shen, C.C. & Huntington, K.W. (2020) Travertine deposits constraining transfer zone neotectonics in geothermal areas: an example from the inner Northern Apennines (Bagno Vignoni-Val d'Orcia area, Italy). *Geothermics*, *85*, article 101763.

Capezzuoli, E., Gandin, A. & Pedley, M. (2014) Decoding tufa and travertine (fresh water carbonates) in the sedimentary record: the state of the art. *Sedimentology*, *61*(1), 1–21.

Carmignani, L., Decandia, F.A., Fantozzi, P.L., Lazzarotto, A., Liotta, D. & Meccheri, M. (1994) Tertiary extensional tectonics in Tuscany (Northern Apennines, Italy). *Tectonophysics*, *238*(1), 295–315.

Carminati, E. & Doglioni, C. (2012) Alps vs. Apennines: the paradigm of a tectonically asymmetric earth. *Earth-Science Reviews*, *112*(1–2), 67–96.

Carucci, V., Petitta, M. & Aravena, R. (2012) Interaction between shallow and deep aquifers in the Tivoli Plain (Central Italy) enhanced by groundwater extraction: a multi-isotope approach and geochemical modeling. *Applied Geochemistry*, *27*(1), 266–280.

Casanova, J. (1994). Stromatolites from the East African rift: a synopsis. In: Bertrand Sarfati, J. & Monty, C. (Eds.) *Phanerozoic stromatolites II*. Dordrecht: Kluwer Academic, pp. 193–226.

Cavinato, G.P. & De Celles, P.G. (1999) Extensional basins in the tectonically bimodal central apennines fold-thrust belt, Italy: response to corner flow above a subducting slab in retrograde motion. *Geology*, *27*(10), 955–958.

Chafetz, H.S. & Folk, R.L. (1984) Travertines: depositional morphology and the bacterially constructed constituents. *Journal of Sedimentary Petrology*, *54*(1), 289–316.

Chafetz, H.S. & Guidry, S.A. (1999) Bacterial shrubs, crystal shrubs, and ray-crystal shrubs: bacterial vs. abiotic precipitation. *Sedimentary Geology*, *126*(1), 57–74.

Chang, K.H. (1975) Unconformity-bounded stratigraphic units. *Geological Society of America Bulletin*, *86*, 1544–1552.

Chilingarian, G.V. & Wolf, K.H. (1994) Diagenesis IV. *Developments in Sedimentology*, *51*, 467.

Claes, H., Degros, M., Soete, J., Claes, S., Kele, S., Mindszenty, A., Török, Á., El Desouky, H., Vanhaecke, F. & Swennen, R. (2017a). Geobody architecture, genesis and petrophysical characteristics of the Budakalász travertines, Buda Hills (Hungary). *Quaternary International*, *437 (Part A)*, 107–128.

Claes, H., Erthal, M., Soete, J., Özkul, M. & Swennen, R. (2017b). Shrub and pore type classification: petrography of travertine shrubs from the Ballık–Belevi area (Denizli, SW Turkey). *Quaternary International, 437 (Part A)*, 147–163.

Claes, H., Soete, J., Van Noten, K., El Desouky, H., Erthal, M., Vanhaecke, F., Özkul, M. & Swennen, R. (2015) Sedimentology, three-dimensional geobody reconstruction and carbon dioxide origin of Pleistocene travertine deposits in the Ballık area (South–West Turkey). *Sedimentology*, *62*(5), 1408–1445.

Claes, H., Török, Á., Soete, J., Mohammadi, Z., Vassilieva, E., Hamaekers, H., Erthal, M.M., Aratman, C., Cheng, H., Edwards, R.L., Shen, C.C., Özkul, M., Kele, S., Mindszenty, A. & Swennen, R. (2020) U/Th dating and open system behavior: implications for travertines based on the study of Süttő (Hungary) and Ballık (Turkey) sites. *Quaternaire. Revue de l'Association française pour l'étude du Quaternaire*, *31*(2), 117–132.

Croci, A., Della Porta, G. & Capezzuoli, E. (2016) Depositional architecture of a mixed travertine–terrigenous system in a fault-controlled continental extensional basin (Messinian, Southern Tuscany, Central Italy). *Sedimentary Geology*, *332*, 13–19.

De Boever, E., Brassier, A., Foubert, A. & Kele, S. (2017a) What do we know about early diagenesis of non-marine carbonates? *Sedimentary Geology*, *361*, 25–51.

De Boever, E., Foubert, A., Lopez, B., Swennen, R., Jaworowski, C., Özkul, M. & Virgone, A. (2017b) Comparative study of the Pleistocene Cakmak quarry (Denizli basin, Turkey) and modern mammoth hot springs deposits (Yellowstone National Park, USA). *Quaternary International*, *437*, 129–146.

De Boever, E., Foubert, A., Oligschlaeger, D., Claes, S., Soete, J., Bertier, P., Özkul, M., Virgone, A. & Swennen, R. (2016) Multiscale approach to (micro) porosity quantification in continental spring carbonate facies: case study from the Cakmak quarry (Denizli, Turkey). *Geochemistry, Geophysics, Geosystems*, *17*(7), 2922–2939.

De Filippis, L., Faccenna, C., Billi, A., Anzalone, E., Brilli, M., Özkul, M., Soligo, M., Tuccimei, P. & Villa, I.M. (2012) Growth of fissure ridge travertines from geothermal springs of Denizli Basin,

western Turkey. *Geological Society of America Bulletin*, *124*(9–10), 1629–1645.

De Filippis, L., Anzalone, E., Billi, A.Faccenna C., Poncia, P.P. & Sella, P. (2013a) The origin and growth of a recently-active fissure ridge travertine over a seismic fault, Tivoli, Italy. *Geomorphology*, *195*, 13–26.

De Filippis, L., Faccenna, C., Billi, A., Anzalone, E., Brilli, M., Soligo, M. & Tuccimei, P. (2013b) Plateau versus fissure ridge travertines from Quaternary geothermal springs of Italy and Turkey: interactions and feedbacks between fluid discharge, paleoclimate, and tectonics. *Earth-Science Reviews*, *123*, 35–52.

De Rita, D., Faccenna, C., Funiciello, R. & Rosa, C. (1995). Structural and geological evolution of the Colli Albani volcanic district. In: Trigila, R. (Ed.) *The volcano of the Alban Hills*. Rome: Tipografia SGS, pp. 33–71.

De Rita, D., Giordano, G., Esposito, A., Fabbri, M. & Rodani, S. (2002) Large volume phreatomagmatic ignimbrites from the Colli Albani volcano (Middle Pleistocene, Italy). *Journal of Volcanology and Geothermal Resources*, *118*, 77–98.

Della Porta, G. (2015). Carbonate build-ups in lacustrine, hydrothermal and fluvial settings: comparing depositional geometry, fabric types and geochemical signature. In: Bosence, D.W.J., Gibbons, K.A., Le Heron, D.P., Morgan, W.A., Pritchard, T. & Vining, B.A. (Eds.) *Microbial carbonates in space and time: implications for global exploration and production*. *Geological Society of London Special Publications*, *418*, 17–68.

Della Porta, G., Capezzuoli, E. & De Bernardo, A. (2017a) Facies character and depositional architecture of hydrothermal travertine slope aprons (Pleistocene, Acquasanta Terme, Central Italy). *Marine and Petroleum Geology*, *87*, 171–187.

Della Porta, G., Croci, A., Marini, M. & Kele, S. (2017b) Depositional architecture, facies character and geochemical signature of the Tivoli travertines (Pleistocene, Acque Albule Basin, Central Italy). *Rivista Italiana di Paleontologia e Stratigrafia*, *123*, 487–540.

Di Salvo, C., Mazza, R. & Capelli, G. (2013) Gli acquiferi in travertino del Lazio: schemi idrogeologici e caratteristiche chimico-fisiche. *Rendiconti Online Società Geologica Italiana*, *27*, 54–76.

Dias, J.L. (2004) A new gas province in South Atlantic Region: recent gas discoveries in Santos Basin, Offshore Brazil. 2004 AAPG International Conference, October 24–27, Cancun, Mexico, 20031.

Dickson, J.A.D. (1966) Carbonate identification and genesis as revealed by staining. *Journal of Sedimentary Research*, *36*(2), 491–505.

Dini, A., Gianelli, G., Puxeddu, M. & Ruggieri, G. (2005) Origin and evolution of Pliocene-Pleistocene granites from the Larderello geothermal field (Tuscan Magmatic Province, Italy). *Lithos*, *81*, 1–31.

Dunham, R.J. (1962) Classification of carbonate rocks according to depositional texture. Classification of Carbonate Rocks. *American Association of Petroleum Geologists Memoir*, *1*, 108–121.

Embry, A.F. & Klovan, E. (1971). A late Devonian reef tract on northeastern Banks Island, N.W.T. *Canadian Society of Petroleum Geologists Bulletin*, *19*, 730–781.

Erthal, M., Capezzuoli, E., Claes, H., Soete, J., Mancini, A. & Swennen, R. (2017) Shrub morpho-type depositional model from Tivoli continental carbonate deposits (Central Italy). *Sedimentary Geology*, *347*, 79–99.

Faccenna, C., Funiciello, R., Bruni, A., Mattei, M. & Sagnotti, L. (1994) Evolution of a transfer related basin: the Ardea basin (Latium, Central Italy). *Basin Resources*, *5*, 1–11.

Faccenna, C., Soligo, M., Billi, A., De Filippis, L., Funiciello, R., Rossetti, C. & Tuccimei, P. (2008) Late Pleistocene depositional cycles of the Lapis Tiburtinus travertine (Tivoli, Central Italy): possible influence of climate and fault activity. *Global and Planetary Change*, *63*, 299–308.

Fouke, B.W. (2011) Hot-spring systems geobiology: abiotic and biotic influences on travertine formation at Mammoth Hot Springs, Yellowstone National Park, USA. *Sedimentology*, *58*(1), 170–219.

Fouke, B.W., Farmer, J.D., Des Marais, D.J., Pratt, L., Sturchio, N.C., Burns, P.C. & Discipulo, M.K. (2000) Depositional facies and aqueous-solid geochemistry of travertine-depositing hot springs (Angel Terrace, Mammoth Hot Springs, Yellowstone National Park, U.S.A.). *Journal of Sedimentary Research. Section A, Sedimentary Petrology and Processes: An International Journal of SEPM (Society for Sedimentary Geology)*, *70*(3), 565–585.

Gaeta, M., Fabrizio, G. & Cavarretta, G. (2000) F-phlogopites in the Alban Hills Volcanic District (Central Italy): indications regarding the role of volatiles in magmatic crystallisation. *Journal of Volcanology and Geothermal Resources*, *99*, 179–193.

Gandin, A. & Capezzuoli, E. (2008) Travertine versus Calcareous tufa: distinctive petrologic features and related stable isotopes signature. Il Quaternario. *Italian Journal of Quaternary Sciences*, *21*, 125–136.

Gandin, A. & Capezzuoli, E. (2014) Travertine: distinctive depositional fabrics of carbonates from thermal spring systems. *Sedimentology*, *61*(1), 264–290.

Giordano, G., De Benedetti, A.A., Diana, A., Diano, G., Esposito, A., Fabbri, M., Gaudioso, F., Marasco, F., Mazzini, I., Miceli, M., Mincione, V., Porreca, M., Rodani, S., Rosa, C., Vinkler, A.P., Caprilli, E., Taviani, S., Trigari, A., Bilardello, D., Malinconico, S., Sabato, C.T., Funiciello, R., Mattei, M., De Rita, D., Parotto, M. & Cas, R.A.F. (2010) Stratigraphy, volcano tectonics and evolution of the Colli Albani volcanic field. *The Colli Albani Volcano*. *Geological Society of London*, *3*(3), 43–97.

Guo, L. & Riding, R. (1992) Aragonite laminae in hot water travertine crusts, Rapolano Terme, Italy. *Sedimentology*, *39*(6), 1067–1079.

Guo, L. & Riding, R. (1994) Origin and diagenesis of Quaternary continental carbonate shrub fabrics Rapolano Terme, central Italy. *Sedimentology*, *41*(3), 499–520.

Guo, L. & Riding, R. (1998) Hot-spring travertine facies and sequences, Late Pleistocene, Rapolano Terme, Italy. *Sedimentology*, *45*(1), 163–180.

Guo, L. & Riding, R. (1999) Rapid facies changes in Holocene fissure ridge hot spring travertines, Rapolano Terme, Italy. *Sedimentology*, *46*(6), 1145–1158.

Janssens, N., Capezzuoli, E., Claes, H., Muchez, P., Yu, T.L., Shen, C.C., Ellam, R.M. & Swennen, R. (2020) Fossil travertine system and its palaeofluid provenance, migration and evolution through time: example from the geothermal area of Acquasanta Terme (Central Italy). *Sedimentary Geology*, *398*, 105580

Jones, B. & Renaut, R.W. (1995) Non-crystallographic calcite dendrites from hot-spring deposits at Lake Bogoria, Kenya. *Journal of Sedimentary Research*, *65*(1a), 154–169.

Jones, B., Renaut, R.W., Owen, R. & Torfason, H. (2005) Growth patterns and implications of complex dendrites in calcite travertines from Lýsuhóll, Snæfellsnes, Iceland. *Sedimentology*, *52*(6), 1277–1301.

Jones, B., Renaut, R.W. & Rosen, M.R. (2000) Trigonal dendritic calcite crystals forming from hot spring waters at Waikite, North Island, New Zealand. *Journal of Sedimentary Research*, *70*(3), 586–603.

Karner, D.B., Marra, F. & Renne, P.R. (2001) The history of the Monti Sabatini and Alban Hills volcanoes: groundwork for assessing

volcanic-tectonic hazards for Rome. *Journal of Volcanology and Geothermal Resources*, *107*, 185–219.

Kitano, Y. (1963) Geochemistry of calcareous deposits found in hot springs. *Journal of Earth Sciences*, *II*, 68–100.

La Vigna, F., Hill, M.C., Rossetto, R. & Mazza, R. (2016) Parameterization, sensitivity analysis, and inversion: an investigation using groundwater modeling of the surface-mined Tivoli-Guidonia basin (Metropolitan City of Rome, Italy). *Hydrogeology Journal*, *24*(6), 1423–1441.

La Vigna, F., Mazza, R. & Capelli, G. (2013a) Water resources in the travertines of Tivoli-Guidonia plain. Numerical modeling as a tool for aquifer management. Le risorse idriche nei travertini della piana di Tivoli-Guidonia. La modellazione numerica come strumento di gestione degli acquiferi. *Rendiconti Online Società Geologica Italiana*, *27*, 77–85.

La Vigna, F., Mazza, R. & Capelli, G. (2013b) Detecting the flow relationships between deep and shallow aquifers in an exploited groundwater system, using long-term monitoring data and quantitative hydrogeology: the Acque Albule basin case (Rome, Italy). *Hydrological Processes*, *27*, 3159–3173.

Liotta, D. (1991) The Arbia-Val Marecchia line, northern Apennines. *Eclogae Geologicae Helvetiae*, *84*, 413–430.

Liotta, D. & Brogi, A. (2020) Pliocene-Quaternary fault kinematics in the Larderello geothermal area (Italy): insights for the interpretation of the present stress field. *Geothermics*, *83*.101714

Maiorani, A., Funiciello, R., Mattei, M. & Turi, B. (1992) Stable isotope geochemistry and structural elements of the Sabina region (Central Apennines, Italy). *Terra Nova*, *4*, 484–488.

Mancini, A., Capezzuoli, E., Erthal, M. & Swennen, R. (2019a) Hierarchical approach to define travertine depositional systems: 3D conceptual morphological model and possible applications. *Marine and Petroleum Geology*, *103*, 549–563.

Mancini, A., Frondini, F., Capezzuoli, E., Galvez, M.E., Lezzi, G., Matarazzi, D., Brogi, A. & Swennen, R. (2019b) Evaluating the geogenic CO_2 flux from geothermal areas by analysing quaternary travertine masses. New data from western central Italy and review of previous CO_2 flux data. *Quaternary Science Review*, *215*, 132–143.

Miall, A.D. (1996) *The Geology of fluvial deposits*. Berlin: Springer Verlag, 582 pp.

Milli, S., Mancini, M., Moscatelli, M., Stigliano, F., Marini, M. & Cavinato, G.P. (2016) From river to shelf, anatomy of a high-frequency depositional sequence: the Late Pleistocene to Holocene Tiber depositional sequence. *Sedimentology*, *63*(7), 1886–1928.

Minissale, A. (2004) Origin, transport and discharge of CO_2 in central Italy. *Earth Science Reviews*, *66*, 89–141.

Minissale, A., Kerrick, D.M., Magro, G., Murrell, M.T., Paldini, M., Rihs, S., Sturchio, N.C., Tassi, F. & Vaselli, O. (2002) Geochemestry of Quaternary travertines in the region north of Rome (Italy): structural, hydrologic and paleoclimatic implications. *Earth and Planetary Science Letters*, *203*, 709–728.

Mohammadi, Z., Claes, H., Capezzuoli, E., Mozafari, M., Soete, J., Aratman, C. & Swennen, R. (2020) Lateral and vertical variations in sedimentology and geochemistry of sub-horizontal laminated travertines (Çakmak quarry, Denizli Basin, Turkey). *Quaternary International*, *540*, 146–168.

Molli, S. (2008) Northern Apennine-Corsica orogenic system: an updated overview. *Geological Society London Special Publications*, *298*(1), 413–442.

Neves, M.A., Morales, N. & Saad, A.R. (2005) Facies analysis of Tertiary alluvial fan deposits in the Jundiaí region, São Paulo, southeastern Brazil. *Journal of South American Earth Sciences*, *19*(4), 513–524.

North American Commission on Stratigraphic Nomenclature (NACSN) (1983) North American stratigraphic code. *American Association of Petroleum Geologists Bulletin*, *67*, 841–875.

Okumura, T., Takashima, C., Shiraishi, F., Akmaluddin, & Kano, A. (2012) Textural transition in an aragonite travertine formed under various flow conditions at Pancuran Pitu, Central Java, Indonesia. *Sedimentary Geology*, *265*, 195–209.

Özkul, M., Varol, B. & Alçiçek, C. (2002) Depositional environments and petrography of Denizli travertines. *Mineral Research and Exploration Bulletin*, *125*, 13–29.

Patacca, E., Sartori, R. & Scandone, P. (1992) Tyrrhenian basin and Apenninic arcs: kinematic relations since late Tortonian times. *Memorie della Società Geolica Italiana*, *45*, 425–451.

Pedley, H.M. & Rogerson, M. (2010) Tufas and speleothems: unravelling the microbial and physical controls. *Geological Society of London*, *336*, 1–5.

Pentecost, A. (2005) *Travertine*. Berlin: Springer-Verlag, pp. 1–448.

Petitta, M., Primavera, P., Tuccimei, P. & Aravena, R. (2010) Interaction between deep and shallow groundwater systems in areas affected by Quaternary tectonics (Central Italy): a geochemical and isotope approach. *Environmental Earth Sciences*, *63*, 11–30.

Rainey, D.K. & Jones, B. (2009) Abiotic versus biotic controls on the development of the Fairmont Hot Springs carbonate deposit, British Columbia, Canada. *Sedimentology*, *56*(6), 1832–1857.

Renaut, R.W., Owen, R.B., Jones, B., Tiercelin, J.J., Tarits, C., Ego, J.K. & Konhauser, K.O. (2013) Impact of lake-level changes on the formation of thermogene travertine in continental rifts: evidence from Lake Bogoria, Kenya Rift Valley. *Sedimentology*, *60*(2), 428–468.

Rezende, M.F. & Pope, M.C. (2015) Importance of depositional texture in pore characterization of subsalt microbialite carbonates, offshore Brazil. *Geological Society of London, Special Publications*, *418*, 1–15.

Ronchi, P. & Cruciani, F. (2015) Continental carbonates as a hydrocarbon reservoir, an analog case study from the travertine of Saturnia, Italy. *AAPG Bulletin*, *99*(4), 711–734.

Rossetti, F., Glodny, J., Theye, T. & Maggi, M. (2015) Pressure-Temperature-deformation-time of the ductile Alpine shearing in Corsica: from orogenic construction to collapse. *Lithos*, *218–219*, 99–116.

Sabato Ceraldi, T. & Green, D. (2016) Evolution of the South Atlantic lacustrine deposits in response to Early Cretaceous rifting, subsidence and lake hydrology. In Sabato, C.T., Hodgkinson, R.A. & Backe, G. (Eds.) *Petroleum geoscience of the West Africa Margin*. *Geological Society of London, Special Publications*, *438*, 77–98.

Saller, A., Rushton, S., Buambua, L., Inman, K., McNeil, R. & Dickson, J.T. (2016) Presalt stratigraphy and depositional systems in the Kwanza Basin, offshore Angola. *AAPG Bulletin*, *100*, 1135–1164.

Serri, G., Innocenti, F. & Manetti, P. (1993) Geochemical and petrological evidence of the subduction of delaminated Adriatic continental lithosphere in the genesis of the Neogene-Quaternary magmatism of Central Italy. *Tectonophysics*, *223*, 117–147.

Soete, J., Kleipool, L.M., Claes, H., Claes, S., Hamaekers, H., Kele, S., Özkul, M., Foubert, A., Reijmer, J.J.G. & Swennen, R. (2015) Acoustic properties in travertines and their relation to porosity and pore types. *Marine and Petroleum Geology*, *59*, 320–335.

Terra, G.J.S., Spadini, A.R., França, A.B., Sombra, C.L., Zambonato, E.E., da Silva Juschaks, L.C., Arienti, L.M., Erthal, M.M., Blauth, M., Franco, M.P., Matsuda, N.S., Carramal da Silva, N.G., Moretti

Júnior, P.A., D'Avila, R.S.F., Schiffer de Souza, R., Tonietto, S.N., Couto dos Anjos, S.M., Campinho, V.S., Winter, W.R., José, G., Terra, S., Leite, C., Costa, L., Goulart, N., Augusto, P., Junior, M., Francisco, R.S., Avila, D., Souza, R.S. & Maria, S. (2010) Carbonate rock classification applied to Brazilian sedimentary basins. *Boletim de Geociencias da Petrobras*, *18*, 9–29.

Toker, E., Kaisery-Özer, M.S., Özkul, M. & Kele, S. (2015) Depositional system and palaeoclimatic interpretations of Middle to Late Pleistocene travertines: Koçabaş, Denizli, south – west Turkey. *Sedimentology*, *62*(5), 1360–1383.

Török, Á., Claes, H., Brogi, A., Liotta, D., Tóth, Á., Mindszenty, A., Kudó, I., Kele, S., Huntington, K.W., Shen, C.C. & Swennen, R. (2019) A multi-methodological approach to reconstruct the configuration of a travertine fissure ridge system: the case of the Cukor quarry (Süttő, Gerecse Hills, Hungary). *Geomorphology*, *345*, 106836

Török, Á., Mindszenty, A., Claes, H., Kele, S., Fodor, L. & Swennen, R. (2017). Geobody architecture of continental carbonates: "Gazda" travertine quarry (Süttő, Gerecse Hills, Hungary). *Quaternary International*, *437* (Part A), 164–185.

Turner, E.C. & Jones, B. (2005) Microscopic calcite dendrites in cold-water tufa: implications for nucleation of micrite and cement. *Sedimentology*, *52*(5), 1043–1066.

Vignaroli, G., Mancini, M., Bucci, F., Cardinali, M., Cavinato, G.P., Moscatelli, M., Putignano, M.L., Sirianni, P., Santangelo, M., Ardizzone, F., Cosentino, G., Di Salvo, C., Fiorucci, F., Gaudiosi, I., Giallini, S., Messina, P., Peronace, E., Polpetta, F., Reichenbach, P., Scionti, V., Simionato, M. & Stigliano, F. (2019) Geology of the central part of the Amatrice Basin (Central Apennines, Italy). *Journal of Maps*, *15*(2), 193–202.

Wright, V.P. (2012) Lacustrine carbonates in rift settings: the interaction of volcanic and microbial processes on carbonate deposition. *Geological Society of London, Special Publications*, *370*(1), 39–47.

Wright, V.P. & Barnett, A. (2015) An abiotic model for the development of textures in some South Atlantic early Cretaceous lacustrine carbonates. In Bosence, D.W.J., Gibbons, K.A., Le Heron, D.P., Morgan, W.A., Pritchard, T. & Vining, B.A. (Eds.) *Microbial carbonates in space and time: implications for global exploration and production*. *Geological Society of London, Special Publications*, *418*, 209–219.

How to cite this article: Scalera, F., Mancini, A., Capezzuoli, E., Claes, H. & Swennen, R. (2022) The role of tectonic activity, topographic gradient and river flood events in the Testina travertine (Acque Albule Basin, Tivoli, Central Italy). *Depositional Record*, 8, 266–291. https://doi.org/10.1002/dep2.155